



di Bernardo, M., Kowalczyk, P. S., & Nordmark, A. (2001). Bifurcations of dynamical systems with sliding : derivation of normal-form mappings.

[Link to publication record in Explore Bristol Research](#)
PDF-document

University of Bristol - Explore Bristol Research

General rights

This document is made available in accordance with publisher policies. Please cite only the published version using the reference above. Full terms of use are available:
<http://www.bristol.ac.uk/pure/about/ebr-terms.html>

Take down policy

Explore Bristol Research is a digital archive and the intention is that deposited content should not be removed. However, if you believe that this version of the work breaches copyright law please contact open-access@bristol.ac.uk and include the following information in your message:

- Your contact details
- Bibliographic details for the item, including a URL
- An outline of the nature of the complaint

On receipt of your message the Open Access Team will immediately investigate your claim, make an initial judgement of the validity of the claim and, where appropriate, withdraw the item in question from public view.

Bifurcations of Dynamical Systems with Sliding: Derivation of normal-form mappings

M. di Bernardo^{*}; P. Kowalczyk^{*†}; A. Nordmark[‡]

December 12, 2001

Abstract

This paper is concerned with the analysis of so-called *sliding bifurcations* in n -dimensional piecewise-smooth dynamical systems with discontinuous vector field. These novel bifurcations occur when the system trajectory interacts with regions on the discontinuity set where sliding is possible. The derivation of appropriate normal form maps is detailed. It is shown that the leading order term in the map depends on the particular bifurcation scenario considered. This is in turn related to the possible bifurcation scenarios exhibited by a periodic orbit undergoing one of the sliding bifurcations discussed in the paper. A third-order relay system serves as a numerical example.

keywords: discontinuous systems; sliding bifurcations; normal form maps; PACS 05.45-a

1 Introduction

Discontinuous events characterise the behaviour of an increasing number of dynamical systems of relevance in applied science and engineering. Examples include the occurrence of impacts in mechanical systems [1], stick-slip motion in oscillators with friction [2], switchings in electronic circuits [3, 4, 5, 6] and hybrid dynamics in control devices [7]. These systems are often modelled by sets of piecewise-smooth (PWS) ordinary differential equations (ODEs). These are smooth in regions G_i of phase space with smoothness being lost as trajectories cross the boundaries $\Sigma_{i,j}$ between adjacent regions, see Fig. 1. Specifically, we have

$$\dot{x} = F(x, t, \mu), \quad (1.1)$$

with $F : \mathbb{R}^{n+m+1} \mapsto \mathbb{R}$ being a piecewise smooth (PWS) vector function; t the time variable; $\mu \in \mathbb{R}^m$ a parameter vector and $x \in \mathbb{R}^n$ the state vector. In each of the phase space regions G_i , the system dynamics are described by a different functional form, F_i , of the system vector field.

Piecewise smooth systems have been shown to exhibit a richness of different dynamical behaviours which include several bifurcations and deterministic chaos [8, 9, 10]. Many of these phenomena are due to the unique nature of these systems and involve interactions between the system trajectories and its phase space boundaries. For example, a dramatic change of the system behaviour is usually observed when a part of the system trajectory hits tangentially one of the boundaries between different regions in phase space. When this occurs the system is said to undergo a *grazing* bifurcation (also known as *C*-bifurcations in the Russian literature)[11, 12, 13, 14, 15]. Grazing phenomena can lead to several dramatic bifurcation scenarios including a sudden transition from stable periodic motion to fully developed chaotic behaviour (e.g. [16, 17]).

^{*}Department of Engineering Mathematics, University of Bristol BS8 1TR U.K. m.dibernardo@bristol.ac.uk

[†]Corresponding Author. Tel. +44(0)117 9289798; fax +44(0)117 9251154 E-mail: p.kowalczyk@bristol.ac.uk

[‡]Department of Mechanics, Royal Institute of Technology, Sweden nordmark@mech.kth.se

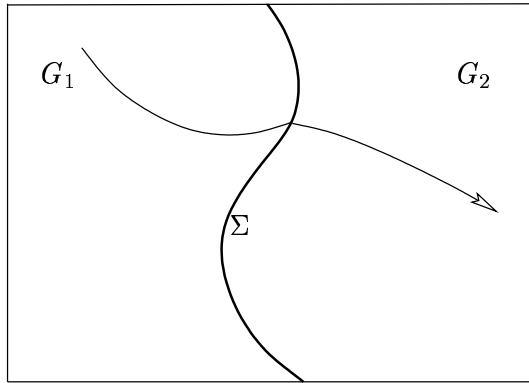


Figure 1: Schematic representation of the system trajectory crossing the boundary, Σ between adjacent regions of smooth dynamics

A particularly intriguing type of solution which is unique to piecewise smooth systems is the so-called sliding or Filippov solution [18]. This is a solution which lies entirely within the discontinuity set of the system under investigation and can be analysed by means of two alternative methods: Filippov Convex method [18] and Utkin equivalent control [19]. Sliding is only possible if the direction of the system vector field on both sides of a discontinuity set points towards the set itself so that nearby trajectories are constrained to evolve on it (see Sec. 3 for further details). Physically, *sliding* motion may be understood as repeated switching between two different system configurations as has been reported in [20, 21, 22].

Recently it has been shown that a novel class of bifurcations can be observed when, as the parameters are varied, the system trajectories cross regions of phase space where sliding is possible (or sliding regions). According to the nature of these intersections and the properties of the vector field describing different scenarios are possible. These bifurcations can explain, for example, the formation of so-called stick-slip dynamics in friction oscillators [23], double spiral bifurcation diagrams in power electronic converters [5] and fast-switching trajectories in relay feedback systems [20].

The occurrence of complex transitions involving sliding was independently observed in the Russian literature [24, 25] and more recently detailed to the case of relay feedback systems in [20]. It was shown that sliding can be associated to four different codimension-1 bifurcation scenarios which are termed (i) sliding bifurcation type I; (ii) multisliding bifurcation; (iii) grazing sliding and (iv) sliding type II (switching sliding) (as will be detailed later in Sec. 3). Extensive numerical simulations were carried out to understand the nature of these four scenarios and some of the complex behaviour they can organise. It was found, for example, that sliding bifurcations can lead to the formation of chaotic attractors and asymmetric orbits in a class of entirely symmetric relay feedback systems [26, 27]. A pressing open problem is the derivation of appropriate normal-form maps for these transitions to allow a proper, consistent classification of these bifurcations.

The aim of this paper is to present for the first time the derivation of such normal-form maps for general n -dimensional piecewise smooth dynamical systems with sliding. Using the concept of discontinuity mapping first introduced in [11] we will present the local analysis of the four sliding bifurcation scenarios mentioned. After giving conditions for sliding to occur, we will briefly describe the main characteristics of these novel bifurcations and give precise conditions for each of them to occur. Using these conditions, we will then derive their normal form maps. In so doing, we will show that sliding bifurcations are indeed novel type of transitions associated to precise functional forms of corresponding normal form maps.

Our aim is to give analytical formulas for the local maps associated with bifurcations involving sliding which can be used to characterise the dynamics of several systems of relevance in applications. As a representative example we will use relay feedback systems which have been extensively studied experimentally.

The paper is outlined as follows. After stating some preliminary hypotheses, the four possible scenarios of sliding bifurcations are presented in Sec. 3. Analytical conditions which must be satisfied at the bifurcation point for each case are given. These conditions are used later in the paper to carry out the analytical derivation of appropriate normal form mappings. These are derived by using the concept of the so-called Zero Time Discontinuity Mapping (ZDM) (see Sec. 4). The detailed derivation of such mapping for each case is outlined in Sec. 5. In Sec. 6 numerical analysis of a third order relay feedback system illustrates the theory presented in the previous section. Finally, in Sec. 7 we briefly discuss the implications of our results to the analysis of periodic orbits undergoing sliding bifurcations, before drawing some conclusions in Sec. 8.

2 Piecewise-Smooth Systems and Sliding Motion

In what follows, we consider a sufficiently small region $D \subset \mathbb{R}^n$ of phase space where we assume that the n -dimensional system (1.1) can be described by the equation

$$\dot{x} = \begin{cases} F_1(x) & \text{if } H(x) > 0 \\ F_2(x) & \text{if } H(x) < 0, \end{cases} \quad (2.2)$$

where $x \in \mathbb{R}^n$, $F_1, F_2 : \mathbb{R}^n \mapsto \mathbb{R}^n$ are sufficiently smooth in D and $H : \mathbb{R}^n \mapsto \mathbb{R}$ is a sufficiently smooth scalar function (at least C^4) of the system states. We label Σ the hyperplane defined by

$$\Sigma := \{x \in \mathbb{R}^n : H(x) = 0\} \quad (2.3)$$

which we term as *switching manifold*. Σ divides D into the two regions

$$G_1 := \{x \in D : H(x) > 0\}, \quad (2.4)$$

and

$$G_2 := \{x \in D : H(x) < 0\}. \quad (2.5)$$

Moreover, we assume that there exists a subset of the switching manifold $\hat{\Sigma} \subset \Sigma$, labelled as *sliding region*, which is simultaneously attracting from both sides in regions G_1 and G_2 . Throughout the neighbourhood of this region we shall assume:

$$\langle \nabla H, F_2 \rangle - \langle \nabla H, F_1 \rangle > 0. \quad (2.6)$$

Under these assumptions, if the system trajectory crosses the sliding region $\hat{\Sigma}$, it is then constrained to evolve within $\hat{\Sigma}$ until it eventually reaches its boundary [18]. This is the so-called *sliding motion* which can be described by considering an appropriate vector field F_s , which lies within the convex hull of F_1 and F_2 , and is tangent to Σ for $x \in \hat{\Sigma}$ [18, 19]. According to Utkin's equivalent control method (see [19] for further details) such vector field is given by

$$F_s = \frac{F_1 + F_2}{2} + H_u(x) \frac{F_2 - F_1}{2}, \quad (2.7)$$

where $H_u(x) \in [-1, 1]$ is some scalar function of the system states. $H_u(x)$ can be obtained in terms of F_1 and F_2 by considering that F_s must be tangential to the switching manifold, i.e. $\langle \nabla H, F_s \rangle = 0$. Using this condition, we then have

$$H_u(x) = -\frac{\langle \nabla H, F_1 \rangle + \langle \nabla H, F_2 \rangle}{\langle \nabla H, F_2 \rangle - \langle \nabla H, F_1 \rangle}. \quad (2.8)$$

We can now define the sliding region $\hat{\Sigma}$ as

$$\hat{\Sigma} := \{x \in \Sigma : -1 \leq H_u(x) \leq 1\}. \quad (2.9)$$

It follows from (2.6) and (2.9) that:

$$\langle \nabla H, F_2 \rangle > 0 > \langle \nabla H, F_1 \rangle, \quad (2.10)$$

throughout the region of interest. Additionally, we define the boundary of the sliding region as $\partial \hat{\Sigma} = \partial \hat{\Sigma}^+ \cup \partial \hat{\Sigma}^-$, where

$$\partial \hat{\Sigma}^+ := \{x \in \Sigma : H_u(x) = 1\}, \quad (2.11)$$

$$\partial \hat{\Sigma}^- := \{x \in \Sigma : H_u(x) = -1\}. \quad (2.12)$$

Note that if $x \in \partial \hat{\Sigma}^+$, from (2.7) we obtain $F_s = F_2$, while, if $x \in \partial \hat{\Sigma}^-$, $F_s = F_1$.

Also, it is worth mentioning here that $H_u(x) = \pm 1$ defines the *equivalent-control* manifold in \mathbb{R}^n whose intersection with Σ determines the boundary of the sliding region $\partial \hat{\Sigma}$. The analysis which is carried on later in the paper assumes that a bifurcation point $x^* = 0$ lies on $\partial \hat{\Sigma}^-$. It should be noted that this assumption places no constraints on the theory presented further on in the paper. ∇H_u is the normal vector to $\partial \hat{\Sigma}^\pm$, which can be expressed as:

$$\begin{aligned} \nabla H_u(x) = & \left[- \left(\frac{\partial H}{\partial x} \frac{\partial F_1}{\partial x} + \frac{\partial^2 H}{\partial x^2} F_1 + \frac{\partial H}{\partial x} \frac{\partial F_2}{\partial x} + \frac{\partial^2 H}{\partial x^2} F_2 \right) \left(\frac{\partial H}{\partial x} F_2 - \frac{\partial H}{\partial x} F_1 \right) \right. \\ & + \left. \left(\frac{\partial H}{\partial x} \frac{\partial F_2}{\partial x} + \frac{\partial^2 H}{\partial x^2} F_2 - \frac{\partial H}{\partial x} \frac{\partial F_1}{\partial x} - \frac{\partial^2 H}{\partial x^2} F_1 \right) \left(\frac{\partial H}{\partial x} F_1 + \frac{\partial H}{\partial x} F_2 \right) \right] \\ & / \left(\frac{\partial H}{\partial x} F_2 - \frac{\partial H}{\partial x} F_1 \right)^2. \end{aligned} \quad (2.13)$$

The dynamics of the system while sliding, which are given by the sliding flow, $\phi_s(x, t)$, generated by F_s , will be moving towards the boundary of the sliding strip, say $\partial \hat{\Sigma}^-$, if $\langle \nabla H_u, F_s \rangle < 0$.

Without loss of generality, we assume that both Σ and $\partial \hat{\Sigma}$ can be flattened by making a series of appropriate near-identity transformations.

In this case, (2.13) becomes

$$\nabla H_u(x) = \frac{- \left(\frac{\partial H}{\partial x} \frac{\partial F_1}{\partial x} + \frac{\partial H}{\partial x} \frac{\partial F_2}{\partial x} \right) \left(\frac{\partial H}{\partial x} F_2 - \frac{\partial H}{\partial x} F_1 \right) + \left(\frac{\partial H}{\partial x} \frac{\partial F_2}{\partial x} - \frac{\partial H}{\partial x} \frac{\partial F_1}{\partial x} \right) \left(\frac{\partial H}{\partial x} F_1 + \frac{\partial H}{\partial x} F_2 \right)}{\left(\frac{\partial H}{\partial x} F_2 - \frac{\partial H}{\partial x} F_1 \right)^2}. \quad (2.14)$$

3 Bifurcations involving sliding

3.1 The four possible cases

We now introduce the possible bifurcation scenarios involving interactions between trajectories of the system and the sliding region $\hat{\Sigma}$. We give a heuristic description of all the possible cases, which we will generically indicate as *sliding bifurcations*. We will then give appropriate analytical conditions characterising each of them in the next section.

According to the results presented in [20], [27, 26] and independently in [24], we can identify four possible cases of bifurcations involving sliding. These can be generalised to the case of n -dimensional piecewise-smooth dynamical systems of the form (2.2). A three-dimensional schematic representation is given in Fig. 2. For the sake of clarity, we can assume that such local bifurcations involve sections of trajectories belonging to some periodic orbit of the system. Figure 2-(a) depicts the scenario we term as **sliding bifurcation** of type I. Here, under parameter variations a part of the system trajectory crosses transversally the boundary of the sliding strip at

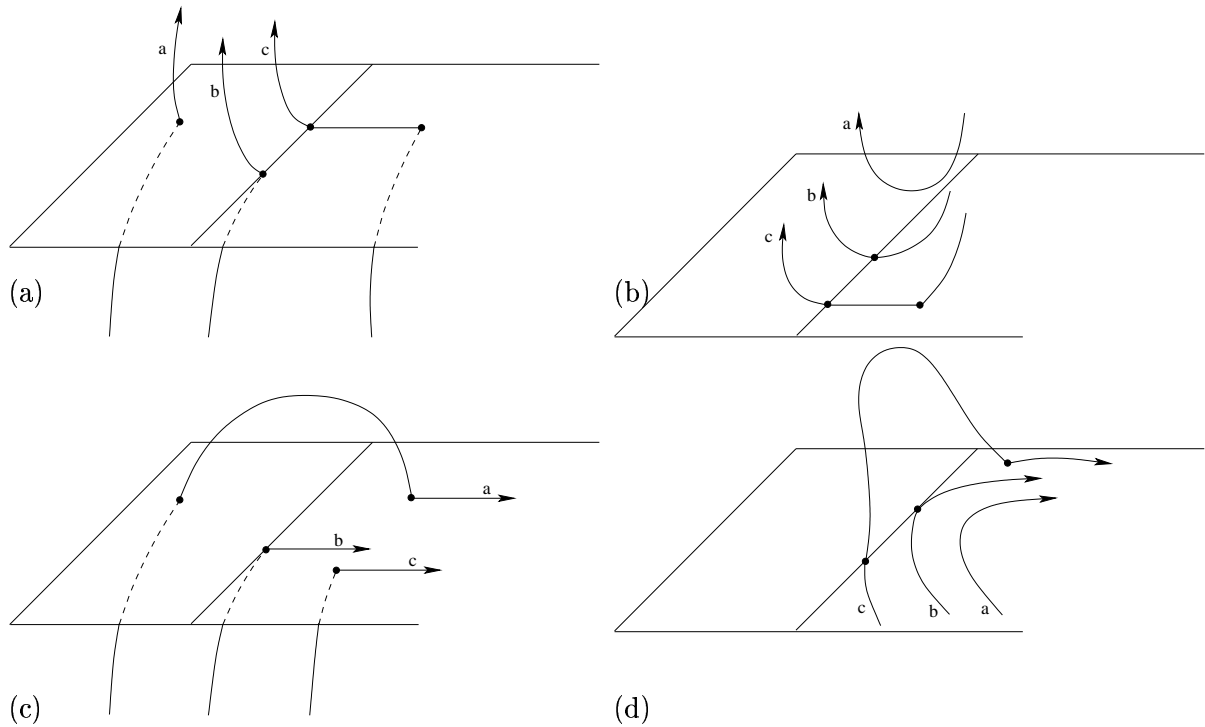


Figure 2: The four possible bifurcation scenarios involving collision of a segment of the trajectory with the boundary of the sliding region $\partial\hat{\Sigma}^-$

the bifurcation point (trajectory labelled b in Fig. 2-(a)). Further variations of the parameter cause the trajectory to enter the sliding region $\hat{\Sigma}$, leading to the onset of sliding motion. Note, that the sliding trajectory then moves locally towards the boundary of $\hat{\Sigma}$. Since, at the boundary $F_s = F_1$ the trajectory leaves the switching manifold tangentially.

In the case presented in Fig. 2-(b), instead, a section of trajectory lying in region G_1 or G_2 grazes the boundary of the sliding region from above (or below). Again, this causes the formation of a section of sliding motion which locally tends to leave $\hat{\Sigma}$. We term this transition as a **grazing-sliding bifurcation**. We note that this transition is the immediate generalisation of so-called grazing bifurcations [11] to dynamical systems with sliding.

A different bifurcation event, which we shall call **sliding bifurcation of type II** or switching-sliding, is depicted in Fig. 2-(c). This scenario is similar to the sliding bifurcation of type I shown in Fig. 2-(a). We see a section of the trajectory crossing transversally the boundary of the sliding region. Now, though, the trajectory stays locally within the sliding region instead of zooming off the switching manifold Σ .

The fourth and last case is the so-called **multisliding bifurcation**, shown in Fig. 2-(d). It differs from the scenarios presented above since the segment of the trajectory which undergoes the bifurcation lies entirely within the sliding region $\hat{\Sigma}$. Namely, as parameters are varied, a sliding section of the system trajectory hits tangentially (grazes) the boundary of the sliding region. Further variations of the parameter cause the formation of an additional segment of trajectory lying above or below the switching manifold, i.e. in region G_1 or G_2 . As shown in [20], this mechanism can give rise to an interesting sliding adding scenario where the accumulation of multisliding bifurcations causes the formation of periodic orbits characterised by an increasing number of sliding sections.

We now make rigorous the scenarios described above by giving analytical conditions for their occurrence.

3.2 Analytical Conditions

In all the cases presented in the previous section, the bifurcation events involve a part of the system trajectory, crossing the boundary of the sliding region $\partial\hat{\Sigma}$. At the bifurcation point, say $x = x^*$, $t = t^*$, the following general conditions must be satisfied for all cases. Specifically, we must have:

1. $H(x^*) = 0$, $\nabla H(x^*) \neq 0$;
2. $H_u(x^*) = -1 \Leftrightarrow F_s = F_1 \Leftrightarrow \langle \nabla H, F_1 \rangle = 0$ at x^* ;

These conditions state that the bifurcation point: (1) belongs to the switching manifold, which is well defined; (2) is located on the boundary of the sliding region (w.l.o.g. we assume it to belong to $\partial\hat{\Sigma}^-$). In what follows we assume, without loss of generality, that the bifurcation point is located at the origin, i.e. $x^* = 0, t^* = 0$. Unless stated otherwise, it is assumed that all the quantities in the equations below are evaluated at the origin.

Using (2.14) and the general conditions for sliding bifurcations, we can now express ∇H_u^* in terms of $\nabla H, F_1, F_2$ as:

$$\nabla H_u^* = -\frac{2}{\langle \nabla H^*, F_2^* \rangle} \nabla H^* \frac{\partial F_1^*}{\partial x} \quad (3.15)$$

where, the superscript $*$ denotes quantities evaluated at the bifurcation point x^* . In the derivations for the sake of brevity we omit the superscript $*$. Note that the denominator of (3.15) is positive, according to (2.6).

3.2.1 Case I: Sliding Bifurcation type I

As shown in Fig 2(a), in this case, the sliding flow moves locally towards the boundary of the sliding region, when perturbed from the bifurcation point. Thus, at the bifurcation point, we must have:

$$\left. \frac{dH_u(\phi_1(0, t))}{dt} \right|_{t=0} < 0, \quad (3.16)$$

which yields the additional condition

$$\langle \nabla H_u, F_1 \rangle < 0. \quad (3.17)$$

After substituting (3.15) for ∇H_u into (3.17) we get:

$$\left. \frac{d^2 H(\phi_1(0, t))}{dt^2} \right|_{t=0} = \langle \nabla H, \frac{\partial F_1}{\partial x} F_1 \rangle > 0. \quad (3.18)$$

3.2.2 Case II: Grazing-Sliding Bifurcation

This scenario is equivalent to Case I (see Fig. 2(b)). When grazing-sliding occurs the sliding flow also moves towards the edge of the sliding strip. Thus, condition (3.18) holds in this case as well.

3.2.3 Case III: Sliding Bifurcation type II (or switching-sliding)

In this case, contrary to what assumed for Case I and II (see Fig. 2(c)), the vector field F_s must point away from the boundary of the sliding region at the bifurcation point. Thus, recalling that along $\partial\hat{\Sigma}$, $F_s = F_1$, we require the extra condition:

$$\left. \frac{dH_u(\phi_1(0, t))}{dt} \right|_{t=0} = \langle \nabla H_u, F_1 \rangle > 0 \Rightarrow \left. \frac{d^2 H(\phi_1(0, t))}{dt^2} \right|_{t=0} = \langle \nabla H, \frac{\partial F_1}{\partial x} F_1 \rangle < 0. \quad (3.19)$$

3.2.4 Case IV: Multisliding Bifurcation

When a multisliding bifurcation occurs, (see Fig. 2(d)) the sliding flow is tangential to the boundary of the sliding strip at the bifurcation point. Hence, we must have

$$\left. \frac{dH_u(\phi_s(0, t))}{dt} \right|_{t=0} = 0 \quad (3.20)$$

and since $F_s = F_1$ along $\partial\hat{\Sigma}^-$, we then have:

$$\langle \nabla H_u, F_s \rangle = \langle \nabla H_u, F_1 \rangle = 0. \quad (3.21)$$

Applying (3.15) for ∇H_u into (3.21) yields:

$$\left. \frac{d^2 H(\phi_1(0, t))}{dt^2} \right|_{t=0} = \langle \nabla H, \frac{\partial F_1}{\partial x} F_1 \rangle = 0. \quad (3.22)$$

Moreover, assuming w.l.o.g. that the sliding flow has a local minimum at the bifurcation point, we also require:

$$\left. \frac{d^2 H_u(\phi_s(0, t))}{dt^2} \right|_{t=0} > 0,$$

i.e.,

$$\left. \frac{d^2 H_u(\phi_s(0, t))}{dt^2} \right|_{t=0} = \frac{\partial H_u}{\partial x} \frac{\partial F_1}{\partial x} F_1 + \frac{\partial^2 H_u}{\partial x^2} F_1 = \langle \nabla H_u, \frac{\partial F_1}{\partial x} F_1 \rangle + \langle \frac{\partial^2 H_u}{\partial x^2}, F_1 \rangle > 0. \quad (3.23)$$

Under the assumption that $\partial\hat{\Sigma}^-$ is flat ((3.23)) becomes:

$$\left. \frac{d^2 H_u(\phi_s(0, t))}{dt^2} \right|_{t=0} = \langle \nabla H_u, \frac{\partial F_1}{\partial x} F_1 \rangle > 0. \quad (3.24)$$

Using (3.15) for ∇H_u , we obtain:

$$\left. \frac{d^3 H(\phi_1(0, t))}{dt^3} \right|_{t=0} = \langle \nabla H, \left(\frac{\partial F_1}{\partial x} \right)^2 F_1 \rangle < 0. \quad (3.25)$$

4 The Discontinuity Mapping

As mentioned in the introduction, the main aim of this paper is that of presenting a comprehensive derivation of appropriate local mappings associated with each of the four sliding bifurcation events for n -dimensional piecewise smooth dynamical systems. For this purpose, we briefly outline here the concept of so-called *discontinuity mappings* which was first introduced in [28]

The discontinuity map can be defined as the correction to be made to trajectories of a piecewise smooth system in order to account for the presence of the switching manifold (see Fig. 3).

Specifically, consider a periodic orbit, of period T , such as the one shown in Fig. 3 and suppose one wishes to construct an appropriate fixed time T -map, say Γ . To do so, say T_1 the time taken by the orbit to go from some point A to its first intersection, B , with the discontinuity boundary, Σ . Then label T_2 the time spent by the orbit on the other side of the boundary and T_3 that needed to get from the exit point C back to A . The trajectory from A back to itself would then be described by the composition of flow Φ_1 and Φ_2 . Namely, one would follow flow Φ_1 for time T_1 , then switch to flow Φ_2 for time T_2 and finally get back to A by considering flow Φ_1 for time T_3 .

Starting from nearby points, one would need to adjust the times in order to take into account correctly the position of the discontinuity boundary. Alternatively, one could keep the flow times

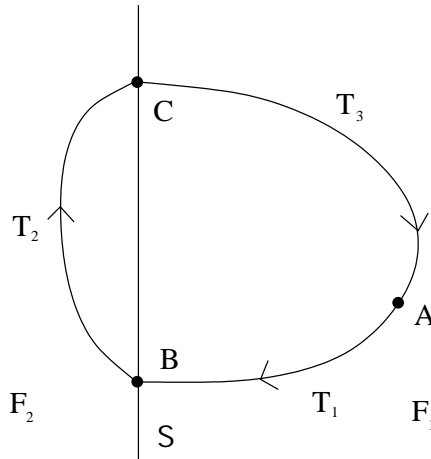


Figure 3: A periodic orbit in a piecewise smooth system

unchanged but consider appropriate corrections. In particular, such correction mappings should be applied between flows Φ_1 and Φ_2 and again between flows Φ_2 and Φ_1 . Namely, the map from a point, x , close to A would then be given by:

$$\Gamma(x) = \Phi_1(\cdot, T_3) \circ DM_{21} \circ \Phi_2(\cdot, T_2) \circ DM_{12} \circ \Phi_1(x, T_1),$$

where DM_{12} and DM_{21} are labelled as *zero-time discontinuity maps* (ZDM). In this sense, the discontinuity map represents the correction brought about by the presence of the switching manifold.

Similarly, if one wants to construct a Poincaré map for a given orbit from some Poincaré section back to itself, similar maps can be introduced which take the name of *Poincaré discontinuity maps* (PDM). Instead of considering fixed times, in this case PDMs introduce appropriate corrections to flows between starting and ending transversal sections (for further details see [29]).

Note that a particular ZDM is applied between a given inflow and a given outflow. It consists, as will be detailed in the rest of the paper, of consecutive flow lines starting with the inflow and ending with the outflow so that the total time is zero. For a PDM, we would start from a section transversal to the inflow and end on a section transversal to the outflow. In particular, a PDM can be constructed out of a ZDM by restricting the initial points to the inflow-section and considering an appropriate projection of the endpoints to the outflow-section. This in turn can be also interpreted as changing the time spent in the outflow, i.e.: instead of achieving zero time (ZDM), we flow until hitting given section (PDM).

These mappings have been shown to be an invaluable tool in characterising bifurcations in piecewise-smooth and discontinuous dynamical systems [28],[30],[31],[29]. As will be shown in the rest of the paper, they can be used to describe analytically the local dynamics of the system at one of the sliding bifurcations described in Sec. 3. In the rest of the paper we shall show that there is a fundamental difference between normal form maps associated with different sliding events.

5 Normal-Form Maps for Sliding Bifurcations

Using the concept of discontinuity map briefly outlined above, we now present the derivation of the normal form maps for each of the four cases discussed in Section 3. In so doing we will assume that the vector fields F_1, F_2, F_s are well defined over the entire phase space region of interest. Therefore, we will suppose that the corresponding flows can be expanded as a Taylor

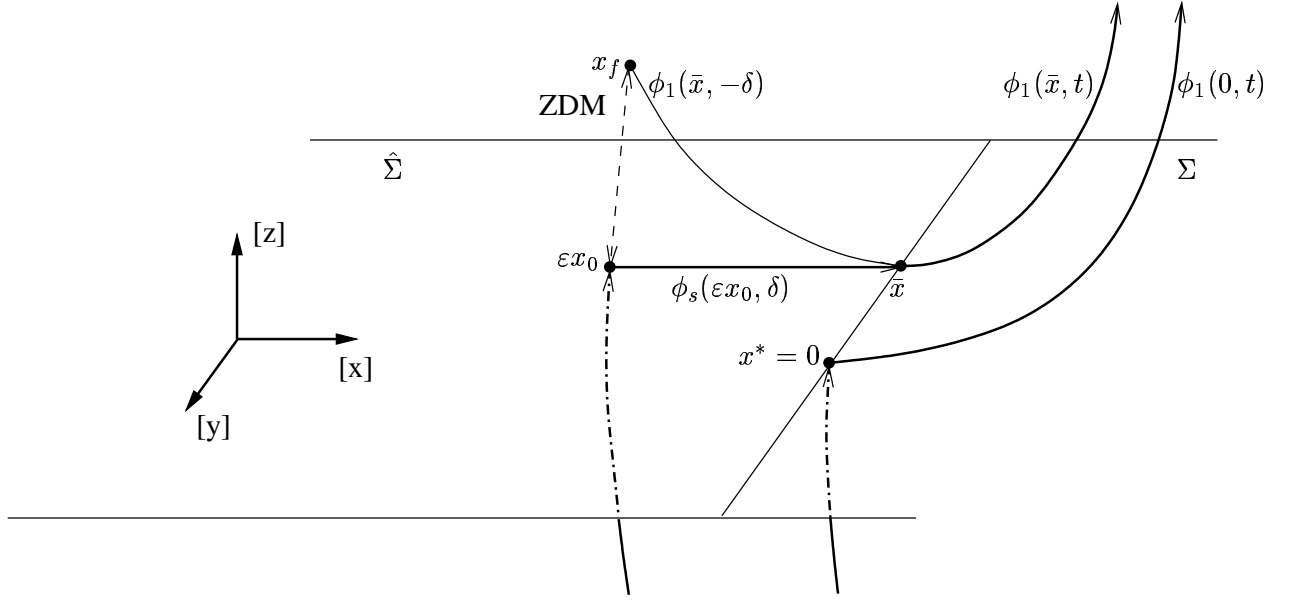


Figure 4: A schematic representation of the ZDM derivation for sliding bifurcations of type I series about the bifurcation point $x^* = 0$, $t^* = 0$ as:

$$\phi_i(x, t) = x + F_i t + a_i t^2 + b_i x t + c_i t^3 + d_i x^2 t + e_i x t^2 + f_i t^4 + g_i x^3 t + h_i x^2 t^2 + j_i x t^3 + \mathcal{O}(5), \quad (5.26)$$

where $i = 1, s$, $\mathcal{O}(5)$ indicates terms of order equal or higher than five and:

$$\begin{aligned} a_i &= \frac{1}{2} \frac{\partial F_i}{\partial x} F_i, & b_i &= \frac{\partial F_i}{\partial x}, & c_i &= \frac{1}{6} \left(\frac{\partial^2 F_i}{\partial x^2} F_i^2 + \left(\frac{\partial F_i}{\partial x} \right)^2 F_i \right), & d_i &= \frac{1}{2} \frac{\partial^2 F_i}{\partial x^2}, \\ e_i &= \frac{1}{2} \left(\frac{\partial^2 F_i}{\partial x^2} F_i + \left(\frac{\partial F_i}{\partial x} \right)^2 \right), & f_i &= \frac{1}{24} \left[\frac{\partial^3 F_i}{\partial x^3} F_i^3 + \frac{\partial^2 F_i}{\partial x^2} \left(F_i \frac{\partial F_i}{\partial x} + \frac{\partial F_i}{\partial x} F_i \right) + \right. \\ &+ \left. \left(\frac{\partial^2 F_i}{\partial x^2} \frac{\partial F_i}{\partial x} + \frac{\partial F_i}{\partial x} \frac{\partial^2 F_i}{\partial x^2} \right) F_i + \left(\frac{\partial F_i}{\partial x} \right)^3 F_i \right], & g_i &= \frac{1}{6} \frac{\partial^3 F_i}{\partial x^3}, & h_i &= \frac{1}{4} \left(\frac{\partial^3 F_i}{\partial x^3} F_i + \frac{\partial F_i}{\partial x} \frac{\partial^2 F_i}{\partial x^2} \right), \\ j_i &= \frac{1}{6} \left[\frac{\partial^3 F_i}{\partial x^3} F_i^2 + \frac{\partial^2 F_i}{\partial x^2} \frac{\partial F_i}{\partial x} F_i + 2 \frac{\partial^2 F_i}{\partial x^2} F_i \frac{\partial F_i}{\partial x} + \frac{\partial F_i}{\partial x} \frac{\partial^2 F_i}{\partial x^2} F_i + \frac{\partial F_i}{\partial x} \right]. \end{aligned} \quad (5.27)$$

Note that we have used a shorthand notation here for the higher-order derivative terms, for example

$$\frac{\partial^3 F_i}{\partial x^3} x^3 = \sum_{i,j,k=1,2,3} \frac{\partial^3 F_i}{\partial x_i x_j x_k} x_i x_j x_k.$$

In what follows, we shall continue to use this shorthand, with care taken to correctly evaluate the derivative tensors when required.

For each case we shall consider ε -perturbations of the bifurcating trajectory, dividing the derivation in different steps.

5.1 Case I: Sliding bifurcation type I

The bifurcation scenario corresponding to this case together with a schematic representation of the map derivation is shown in fig. 4. Here we can see the bifurcating trajectory $\phi_1(0, t)$ crossing $\hat{\Sigma}$ at the point $x^* = 0$ lying on its boundary $\partial \hat{\Sigma}^-$. In order to derive the ZDM, we consider a perturbation of the bifurcating trajectory such that the new trajectory hits the sliding region

$\hat{\Sigma}$ at some point, say $\varepsilon x_0 \in \hat{\Sigma}$. The trajectory is then constrained to evolve within $\hat{\Sigma}$ following the *sliding* flow $\phi_s(\varepsilon x_0, t)$. Under condition (3.18), the system evolution hits the boundary of the sliding region $\hat{\Sigma}$ after some time, say δ , at the point $\bar{x} := \phi_s(\varepsilon x_0, \delta)$. The system evolution then leaves the plane following $\phi_1(\bar{x}, t)$.

The zero-time discontinuity mapping or ZDM in this context is the correction that needs to be applied to the flow at point εx_0 in order to account for the presence of the sliding region. Specifically, this correction must be such that the system evolution across the surface may be described entirely by applying the discontinuity map and using flow ϕ_1 . As depicted in Fig. 4, the ZDM maps εx_0 to some point, say x_f . From x_f the trajectory then evolves through \bar{x} following flow ϕ_1 . Thus, all the important information concerning the presence of the switching manifold $\hat{\Sigma}$ and its influence is indeed captured by the ZDM.

Our aim is to get an analytical expression for the ZDM. To do so we shall proceed in two steps: (i) we evaluate the trajectory from the point εx_0 to the point \bar{x} following ϕ_s for time δ ; (ii) starting from \bar{x} we follow ϕ_1 backward in time for the same amount of time as in (i), reaching the final point x_f . Note that the elapsed time from εx_0 to x_f equals 0.

5.1.1 First step

Let $x_m(t) = \phi_1(0, t)$ be the bifurcating trajectory and let us consider perturbations of x_m of size ε :

$$x(t) = \phi_s(\varepsilon x_0, t) \quad (5.28)$$

for some x_0 which we assume to be such that:

$$\langle \nabla H_u, x_0 \rangle > 0 \quad (5.29)$$

The condition above ensures that for $\varepsilon > 0$ we analyse the trajectory which crosses the switching manifold within the sliding region $\hat{\Sigma}$. If $\varepsilon > 0$, then at some time $t_1 = \delta$ the perturbed trajectory, $x(t)$, will cross the boundary of the sliding region $\hat{\Sigma}$ at $x = \bar{x}$ given by:

$$\begin{aligned} \bar{x} &= \phi_s(\varepsilon x_0, \delta) \approx \varepsilon x_0 + \delta F_s + \delta^2 a_s + \varepsilon \delta b_s x_0 + \delta^3 c_s + \varepsilon^2 \delta d_s x_0^2 \\ &\quad + \varepsilon \delta^2 e_s x_0 + \delta^4 f_s + \varepsilon^3 \delta g_s x_0^3 + \varepsilon^2 \delta^2 h_s x_0^2 + \varepsilon \delta^3 j_s x_0. \end{aligned} \quad (5.30)$$

We wish to define δ to be the time such that $H_u(\bar{x}) = 0$ which, since $\partial \hat{\Sigma}^-$ and Σ are flat to leading order, implies:

$$\langle \nabla H_u, \bar{x} \rangle = 0 \quad (5.31)$$

Using (5.30) for \bar{x} , (5.31) becomes:

$$\begin{aligned} \varepsilon x_0 H_u + \delta F_s H_u + \delta^2 a_s H_u + \varepsilon \delta (b_s x_0) H_u + \delta^3 c_s H_u + \varepsilon^2 \delta (d_s x_0^2) H_u + \varepsilon \delta^2 (e_s x_0) H_u \\ + \delta^4 f_s H_u + \varepsilon^3 \delta (g_s x_0^3) H_u + \varepsilon^2 \delta^2 (h_s x_0^2) H_u + \varepsilon \delta^3 (j_s x_0) H_u \approx 0, \end{aligned} \quad (5.32)$$

where the subscript H_u denotes the component of a vector quantity along ∇H_u i.e.

$$Y_{H_u} = \langle \nabla H_u, Y \rangle. \quad (5.33)$$

We solve (5.32) for δ as an asymptotic expansion in ε . To establish a leading order term of the asymptotic expansion we will balance the first and the second term of (5.32). This gives the asymptotic expansion with the leading order term of $\mathcal{O}(\varepsilon)$. Solving (5.32) for δ as an asymptotic expansion in ε with the lowest term of order $\mathcal{O}(\varepsilon)$ gives:

$$\delta = \gamma_1 \varepsilon + \gamma_2 \varepsilon^2 + \gamma_3 \varepsilon^3 + \mathcal{O}(\varepsilon^4). \quad (5.34)$$

After substituting (5.34) into (5.32) and solving for coefficients: $\gamma_1, \gamma_2, \gamma_3$ we get:

$$\gamma_1 = -\frac{\langle \nabla H_u, x_0 \rangle}{\langle \nabla H_u, F_s \rangle} \quad (5.35)$$

$$\gamma_2 = -\frac{\gamma_1^2 \langle \nabla H_u, a_s \rangle + \gamma_1 \langle \nabla H_u, b_s x_0 \rangle}{\langle \nabla H_u, F_s \rangle} \quad (5.36)$$

$$\begin{aligned} \gamma_3 = & -\frac{(\gamma_2 \langle \nabla H_u, b_s x_0 \rangle + \gamma_1 \langle \nabla H_u, d_s x_0^2 \rangle + \gamma_1^3 \langle \nabla H_u, c_s \rangle +} \\ & \frac{+ 2\gamma_1 \gamma_2 \langle \nabla H_u, a_s \rangle + \gamma_1^2 \langle \nabla H_u, e_s x_0 \rangle)}{\langle \nabla H_u, F_s \rangle} \end{aligned} \quad (5.37)$$

Since condition (3.16) for sliding type I demands the denominator of (5.35) to be negative and the numerator of (5.35) to be positive (condition (5.29)), γ_1 is positive. Thus, our asymptotic expansion is consistent. After substituting (5.34) into (5.30), we get also the following leading-order expression for \bar{x} :

$$\bar{x} = \varepsilon \chi_1 + \varepsilon^2 \chi_2 + \varepsilon^3 \chi_3 \quad (5.38)$$

where:

$$\chi_1 = x_0 + \gamma_1 F_s, \quad (5.39)$$

$$\chi_2 = \gamma_2 F_s + \gamma_1^2 a_s + \gamma_1 b_s x_0, \quad (5.40)$$

$$\chi_3 = \gamma_3 F_s + x_0^2 \gamma_1 d_s + \gamma_1^3 c_s + 2\gamma_1 \gamma_2 a_s + \gamma_2 b_s x_0 + x_0 e_s \gamma_1^2. \quad (5.41)$$

$$(5.42)$$

5.1.2 Second step

We now have to consider the evolution of the perturbed trajectory backward in time from the point \bar{x} to some final point x_f , defined as:

$$\begin{aligned} x_f = & \phi_1(\bar{x}, -\delta) \approx \bar{x} - \delta F_1 + \delta^2 a_1 - \delta b_1 \bar{x} - \delta^3 c_1 - \\ & \delta \bar{x}^2 d_1 + \bar{x} \delta^2 e_1 + \delta^4 f_1 - \bar{x}^3 \delta g_1 + \delta^2 h_1 \bar{x}^2 - \bar{x} \delta^3 j_1. \end{aligned} \quad (5.43)$$

Substituting (5.34) and (5.38) into (5.43), we can express x_f in terms of the initial perturbation ε . Collecting terms at subsequent powers of ε yields the following expression:

$$x_f = (\chi_1 - \gamma_1 F_1) \varepsilon + (\chi_2 + \gamma_1^2 a_1 - \gamma_2 F_1 - \chi_1 \gamma_1 b_1) \varepsilon^2 + \mathcal{O}(\varepsilon^3). \quad (5.44)$$

Let us substitute (5.39) and (5.40) for χ_1 and χ_2 , respectively. After carrying out simplifications we get the following expression for x_f to leading order:

$$x_f = \varepsilon x_0 - \frac{1}{4} \frac{\langle \nabla H_u, x_0 \rangle^2}{\langle \nabla H_u, F_1 \rangle} (F_2 - F_1) \varepsilon^2. \quad (5.45)$$

Thus, the ZDM for sliding type I can be written as:

$$D(x_0) = \begin{cases} \varepsilon x_0 & \text{if } \langle \nabla H_u, x_0 \rangle \leq 0 \\ \varepsilon x_0 + \varepsilon^2 \mathbf{v} + \mathcal{O}(\varepsilon^3) & \text{if } \langle \nabla H_u, x_0 \rangle > 0 \end{cases}, \quad (5.46)$$

where:

$$\mathbf{v} = -\frac{1}{4} \frac{\langle \nabla H_u, x_0 \rangle^2}{\langle \nabla H_u, F_1 \rangle} (F_2 - F_1). \quad (5.47)$$

This condition ensures that the perturbed trajectory crosses Σ (twice) close to x^* . In fact, this is equivalent to leading order to requiring that the trajectory has a negative local minimum value near the origin as such a minimum value is given by:

$$\varepsilon \langle \nabla H, x_0 \rangle + \mathcal{O}(\varepsilon^2). \quad (5.51)$$

Under these conditions, if $\varepsilon > 0$ is sufficiently small there exists some time $t_1 = -\delta$ such that the trajectory, $x(t)$, crosses the switching manifold Σ at a point \bar{x} within the sliding region $\hat{\Sigma}$.

Specifically, \bar{x} , will be given by:

$$\begin{aligned} \bar{x} &= \phi_1(\varepsilon x_0, -\delta) \approx \varepsilon x_0 - \delta F_1 + \delta^2 a_1 - \varepsilon \delta b_1 x_0 - \delta^3 c_1 - \varepsilon^2 \delta d_1 x_0^2 \\ &\quad + \varepsilon \delta^2 e_1 x_0 + \delta^4 f_1 - \varepsilon^3 \delta g_1 x_0^3 + \varepsilon^2 \delta^2 h_1 x_0^2 - \varepsilon \delta^3 j_1 x_0. \end{aligned} \quad (5.52)$$

We wish to define δ to be the time such that $H(\bar{x}) = 0$, which since $H(0) = 0$ and Σ is flat, implies:

$$\langle \nabla H, \bar{x} \rangle = 0. \quad (5.53)$$

Using (5.52) for \bar{x} , (5.53) yields to leading order:

$$\begin{aligned} \varepsilon x_{0H} - \delta F_{1H} + \delta^2 a_{1H} - \varepsilon \delta (b_1 x_0)_H - \delta^3 c_{1H} - \varepsilon^2 \delta (d_1 x_0^2)_H + \varepsilon \delta^2 (e_1 x_0)_H \\ + \delta^4 f_{1H} - \varepsilon^3 \delta (g_1 x_0^3)_H + \varepsilon^2 \delta^2 (h_1 x_0^2)_H - \varepsilon \delta^3 (j_1 x_0)_H \approx 0 \end{aligned} \quad (5.54)$$

We note that second term in (5.54) is nought since condition (3.18) yields $\langle \nabla H, F_1 \rangle = 0$. Solving (5.54) for δ as an asymptotic expansion in $\sqrt{\varepsilon}$ gives:

$$\delta = \gamma_1 \sqrt{\varepsilon} + \gamma_2 \varepsilon + \gamma_3 \varepsilon^{3/2} + \mathcal{O}(\varepsilon^2). \quad (5.55)$$

Substituting (5.55) into (5.54) and solving for $\gamma_1, \gamma_2, \gamma_3$, we get:

$$\gamma_1 = \sqrt{\frac{-x_{0H}}{a_{1H}}} = \sqrt{-2 \frac{\langle \nabla H, x_0 \rangle}{\langle \nabla H, \frac{\partial F_1}{\partial x} F_1 \rangle}}, \quad (5.56)$$

$$\gamma_2 = \frac{1}{2} \frac{\gamma_1^2 c_{1H} + (b_1 x_0)_H}{a_{1H}}, \quad (5.57)$$

$$\gamma_3 = \frac{1}{2} \frac{-\gamma_2^2 a_{1H} - \gamma_1^2 (x_0 e_1)_H + \gamma_2 (b_1 x_0)_H + 3\gamma_1^2 \gamma_2 c_{1H} - \gamma_1^4 f_{1H}}{\gamma_1 a_{1H}}. \quad (5.58)$$

Finally, substituting (5.55)–(5.58) into (5.98) and collecting terms at subsequent powers of $\sqrt{\varepsilon}$, we obtain:

$$\bar{x} = \chi_1 \sqrt{\varepsilon} + \chi_2 \varepsilon + \chi_3 \varepsilon^{3/2} + \mathcal{O}(\varepsilon^2), \quad (5.59)$$

where:

$$\chi_1 = -\gamma_1 F_1, \quad (5.60)$$

$$\chi_2 = x_0 - \gamma_2 F_1 + \gamma_1^2 a_1, \quad (5.61)$$

$$\chi_3 = -\gamma_3 F_1 + 2\gamma_1 \gamma_2 a_1 - \gamma_1^3 c_1 - \gamma_1 b_1 x_0. \quad (5.62)$$

5.2.2 Second step

Having derived an expression for \bar{x} , we need to consider now the subsequent sliding motion along $\hat{\Sigma}$. In particular, the system trajectory starting from \bar{x} will be constrained to evolve along the sliding manifold for some time, say Δ , until reaching its boundary at the point \hat{x} .

Using again Taylor series expansion, we can get an approximate expression for $\hat{x} = \phi_s(\bar{x}, \Delta)$ as:

$$\begin{aligned}\hat{x} \approx & \bar{x} + \Delta F_s + \Delta^2 a_s + \Delta b_s \bar{x} + \Delta^3 c_s + \Delta d_s \bar{x}^2 \\ & + \Delta^2 e_s \bar{x} + \Delta^4 f_s + \Delta g_s \bar{x}^3 + \Delta^2 h_s \bar{x}^2 + \Delta^3 j_s \bar{x}.\end{aligned}\quad (5.63)$$

Now, since \hat{x} lies on the boundary of the sliding region, $\partial\hat{\Sigma}^-$, the following condition must hold:

$$\langle \nabla H_u, \hat{x} \rangle = 0. \quad (5.64)$$

Applying (5.64) to (5.63) we get:

$$\begin{aligned}\bar{x}_{H_u} + \Delta F_{sH_u} + \Delta^2 a_{sH_u} + \Delta (b_s \bar{x})_{H_u} + \Delta^3 c_{sH_u} + \Delta (d_s \bar{x}^2)_{H_u} \\ + (\Delta^2 e_s \bar{x})_{H_u} + \Delta^4 f_{sH_u} + \Delta (g_s \bar{x}^3)_{H_u} + \Delta^2 (h_s \bar{x}^2)_{H_u} + \Delta^3 (j_s \bar{x})_{H_u} \approx 0.\end{aligned}$$

Solving (5.65) for Δ as an asymptotic expansion in $\sqrt{\varepsilon}$, ignoring the trivial solution $\Delta = 0$, we obtain:

$$\Delta = \nu_1 \sqrt{\varepsilon} + \nu_2 \varepsilon + \nu_3 \varepsilon^{3/2}, \quad (5.65)$$

where:

$$\nu_1 = \gamma_1, \quad (5.66)$$

$$\nu_2 = -\frac{\chi_{2H_u} + \nu_{1H_u}^2 a_{sH_u} + \chi_{1H_u} \nu_1 b_{sH_u}}{F_{sH_u}}, \quad (5.67)$$

$$\begin{aligned}\nu_3 = & -\frac{(\chi_{1H_u}^2 d_s)_{H_u} \nu_1 + \chi_{3H_u} + (b_s \chi_{1H_u})_{H_u} \nu_2 + (b_s \chi_{2H_u})_{H_u} \nu_1}{F_{sH_u}} + \\ & + \frac{(\chi_{1H_u} e_s)_{H_u} \nu_1^2 + 2\nu_{1H_u} \nu_2 a_{sH_u} + \nu_{1H_u}^3 c_{sH_u}}{F_{sH_u}}\end{aligned}\quad (5.68)$$

5.2.3 Third step

The last step describes the evolution of the trajectory from \hat{x} to the point x_f obtained by considering flow ϕ_1 backward in time. Specifically, we have:

$$\begin{aligned}x_f = & \phi_1(\hat{x}, \delta - \Delta) \approx \hat{x} + (\delta - \Delta) F_1 + (\delta - \Delta)^2 a_1 + (\delta - \Delta) b_1 \hat{x} + (\delta - \Delta)^3 c_1 + \hat{x}^2 (\delta - \Delta) d_1 \\ & + \hat{x} (\delta - \Delta)^2 e_1 + (\delta - \Delta)^4 f_1 + \hat{x}^3 (\delta - \Delta) g_1 + (\delta - \Delta)^2 h_1 \hat{x}^2 + \hat{x} (\delta - \Delta)^3 j_1.\end{aligned}\quad (5.69)$$

Substituting (5.55), (5.59), (5.63), (5.65) into (5.69), we can express x_f in terms of the initial perturbation ε . Namely, collecting terms at subsequent powers of $\sqrt{\varepsilon}$ yields:

$$\begin{aligned}x_f = & (\chi_1 + \nu_1 F_s (\gamma_1 - \nu_1) F_1) \sqrt{\varepsilon} + (\chi_2 + a_s \nu_1^2 + \nu_2 F_s + \\ & (\gamma_1 - \nu_1) b_1 (\chi_1 + \nu_1 F_s) + (\gamma_1 - \nu_1)^2 a_1 + (\gamma_2 - \nu_2) F_1 + b_s \chi_1 \nu_1) \varepsilon + \mathcal{O}(\varepsilon^{3/2}).\end{aligned}\quad (5.70)$$

Since, according to (5.60) and (5.66), $\nu_1 = \gamma_1$ and $\chi_1 = \gamma_1 F_1$ then the term at $\sqrt{\varepsilon}$ simplifies to 0. Moreover, using (5.60), (5.61) and (5.66), we get:

$$x_f \approx (\gamma_1^2 a_1 + x_0 - b_s \gamma_1^2 F_1 + a_s \gamma_1^2) \varepsilon. \quad (5.71)$$

which, after some further algebraic manipulations, yields to leading order:

$$x_f = \varepsilon x_0 - \left(\frac{\langle \nabla H, x_0 \rangle}{\langle \nabla H, F_2 \rangle} (F_2 - F_1) \right) \varepsilon + \mathcal{O}(\varepsilon^{3/2}). \quad (5.72)$$

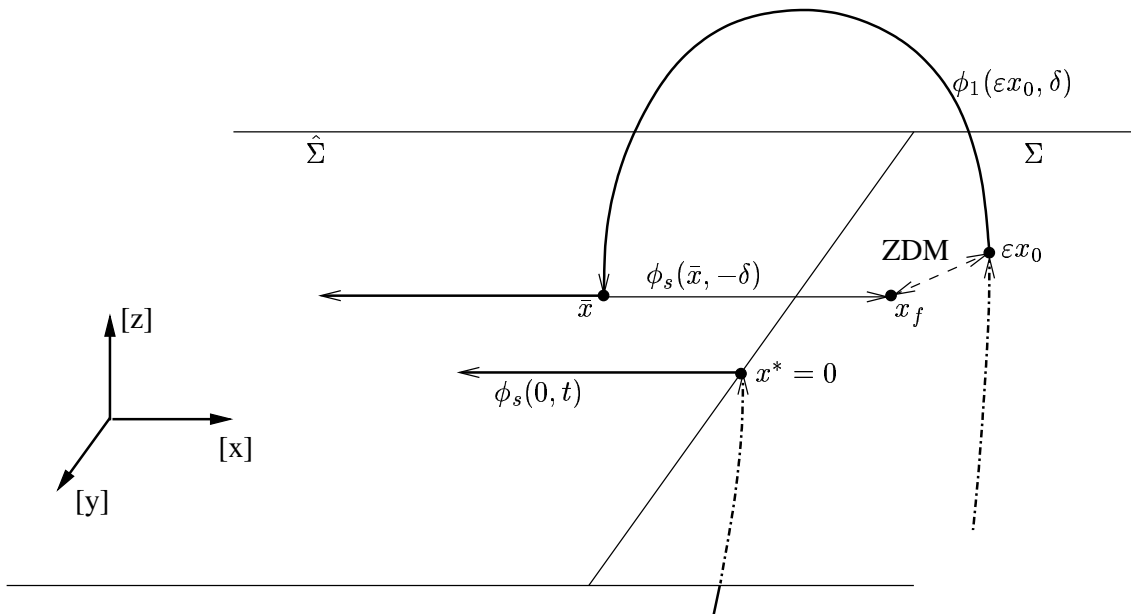


Figure 6: A schematic representation of constructing the ZDM for the sliding bifurcation type II.

Under our assumptions, $F_1 \neq F_2$, $\langle \nabla H, F_2 \rangle > 0$ and, according to (5.50), $\langle \nabla H, x_0 \rangle < 0$. Hence, (5.72) is non-zero and well-defined.

In conclusion, the local normal-form map associated to a grazing sliding bifurcation is piecewise-linear and can be written in the form:

$$D(x_0) = \begin{cases} \varepsilon x_0 & \text{if } \langle \nabla H, x_0 \rangle \geq 0 \\ \varepsilon x_0 + \varepsilon \mathbf{v} + \mathcal{O}(\varepsilon^{3/2}) & \text{if } \langle \nabla H, x_0 \rangle < 0 \end{cases}, \quad (5.73)$$

where

$$\mathbf{v} = -\frac{\langle \nabla H, x_0 \rangle}{\langle \nabla H, F_2 \rangle} (F_2 - F_1). \quad (5.74)$$

5.3 Case III: sliding bifurcation type II

In the switching-sliding bifurcation scenario, the bifurcating trajectory is characterised by hitting the sliding region on its boundary and then sliding away from it along the switching manifold (see Fig. 6). Let us consider a new trajectory hitting the switching manifold outside the sliding region in the neighbourhood of the point x^* . Let's say εx_0 the point at which the new trajectory is rooted. The ZDM in this case represents the correction that must be taken into account in order to describe locally the entire trajectory using just the sliding flow ϕ_s . The analytical construction of the ZDM proceeds in two steps: (i) firstly we consider the system evolution from εx_0 using flow ϕ_1 until it reaches the sliding region at the point \bar{x} after some time δ ; (ii) then we flow backwards in time for the same amount of time from the point \bar{x} using the sliding flow ϕ_s . As usual, the ZDM is then the mapping from εx_0 to x_f .

5.3.1 First step

Let $x_m(t) = \phi_s(0, t)$ be the trajectory which undergoes a sliding bifurcation type II. We consider ε -perturbations of $x_m(t)$ of the form:

$$x(t) = \phi_s(\varepsilon x_0, t), \quad (5.75)$$

for some x_0 which we assume to be such that:

$$\langle \nabla H_u, x_0 \rangle < 0. \quad (5.76)$$

Condition (5.76) ensures that, for $\varepsilon > 0$, the trajectory crosses the switching manifold within the sliding region $\hat{\Sigma}$.

Firstly, we evaluate the flow ϕ_1 from the point εx_0 until its first intersection with the sliding region, say \bar{x} . Assume such intersection to take place after some time δ , we have:

$$\begin{aligned}\bar{x} &= \phi_1(\varepsilon x_0, \delta) \approx \varepsilon x_0 + \delta F_1 + \delta^2 a_1 + \varepsilon \delta b_1 x_0 + \delta^3 c_1 + \varepsilon^2 \delta d_1 x_0^2 \\ &\quad + \varepsilon \delta^2 e_1 x_0 + \delta^4 f_1 + \varepsilon^3 \delta g_1 x_0^3 + \varepsilon^2 \delta^2 h_1 x_0^2 + \varepsilon \delta^3 j_1 x_0.\end{aligned}\quad (5.77)$$

We wish to define δ to be the time such that $H(\bar{x}) = 0$, which since $H(0) = 0$ and Σ is flat, implies:

$$\langle \nabla H, \bar{x} \rangle = 0. \quad (5.78)$$

Using (5.77) for \bar{x} , (5.78) yields that to leading order:

$$\begin{aligned}\varepsilon x_{0H} + \delta F_{1H} + \delta^2 a_{1H} + \varepsilon \delta (b_1 x_0)_H + \delta^3 c_{1H} + \varepsilon^2 \delta (d_1 x_0^2)_H + \varepsilon \delta^2 (e_1 x_0)_H \\ + \delta^4 f_{1H} + \varepsilon^3 \delta (g_1 x_0^3)_H + \varepsilon^2 \delta^2 (h_1 x_0^2)_H + \varepsilon \delta^3 (j_1 x_0)_H = 0.\end{aligned}\quad (5.79)$$

The first term in (5.79) disappears since the point x_0 lies on the switching manifold by definition. Moreover, at the bifurcation point, we also have $\langle \nabla H, F_1 \rangle = 0$, thus the second term of (5.79) vanishes.

Solving (5.79) for δ as an asymptotic expansion in ε with the lowest term of $\mathcal{O}(\varepsilon)$ gives:

$$\delta = \gamma_1 \varepsilon + \gamma_2 \varepsilon^2 + \gamma_3 \varepsilon^3 + \mathcal{O}(\varepsilon^4), \quad (5.80)$$

where:

$$\gamma_1 = -2 \frac{\langle \nabla H_u, x_0 \rangle}{\langle \nabla H_u, F_s \rangle}, \quad (5.81)$$

$$\gamma_2 = -\frac{\gamma_1 ((d_1 x_0^2)_H + \gamma_1^2 c_{1H} + (e_1 x_0)_H \gamma_1)}{(2\gamma_1 a_1 + (b_1 x_0)_H)}, \quad (5.82)$$

$$\begin{aligned}\gamma_3 &= -\frac{\gamma_2 (d_1 x_0^2)_H + (h_1 x_0^2)_H \gamma_1^2 + g_1 x_0^3 \gamma_1 + 3\gamma_1^2 \gamma_2 c_{1H}}{(b_1 x_0)_H + 2\gamma_1 a_{1H}} + \\ &\quad - \frac{\gamma_2^2 a_{1H} + \gamma_1^4 f_{1H} + 2(e_1 x_0)_H \gamma_1 \gamma_2 + \gamma_1^3 (x_0 j_1)_H}{(b_1 x_0)_H + 2\gamma_1 a_{1H}}.\end{aligned}\quad (5.83)$$

Note that the analytical conditions for the sliding bifurcation type II, Eq. (3.19), guarantee that such asymptotic expansion is consistent.

Finally, substituting (5.80) into (5.77), we get the following expression for \bar{x} (we shall consider terms up to third order):

$$\bar{x} = \varepsilon \chi_1 + \varepsilon^2 \chi_2 + \varepsilon^3 \chi_3, \quad (5.84)$$

where:

$$\chi_1 = x_0 + \gamma_1 F_1, \quad (5.85)$$

$$\chi_2 = \gamma_2 F_1 + \gamma_1^2 a_1 + \gamma_1 b_1 x_0, \quad (5.86)$$

$$\chi_3 = \gamma_3 F_1 + x_0^2 \gamma_1 d_1 + \gamma_1^3 c_1 + 2\gamma_1 \gamma_2 a_1 + x_0 \gamma_2 b_1 + x_0 e_1 \gamma_1^2. \quad (5.87)$$

$$(5.88)$$

5.3.2 Second step

To obtain the ZDM, we now have to solve the system backward in time using flow ϕ_s , starting from \bar{x} for time $-\delta$. Using again appropriate Taylor series expansions, we get:

$$\begin{aligned} x_f = \phi_s(\bar{x}, -\delta) &\approx \bar{x} - \delta F_s + \delta^2 a_s - \delta b_s \bar{x} - \delta^3 c_s - \delta \bar{x}^2 d_s \\ &\quad + \bar{x} \delta^2 e_s + \delta^4 f_s - \bar{x}^3 \delta g_s + \delta^2 h_s \bar{x}^2 - \bar{x} \delta^3 j_s. \end{aligned} \quad (5.89)$$

Using (5.80), (5.84), we can then express x_f in terms of the initial perturbation ε . Namely, collecting terms up to third order yields:

$$\begin{aligned} x_f = & (\chi_1 - \gamma_1 F_s) \varepsilon + (\chi_2 + \gamma_1^2 a_s - \gamma_2 F_s - \chi_1 \gamma_1 b_s) \varepsilon^2 \\ & + (-\gamma_3 F_s + \chi_3 - (\chi_1 \gamma_2 + \chi_2 \gamma_1) b_s + \chi_1 \gamma_1^2 e_s - \chi_1^2 d_s \gamma_1 + 2\gamma_1 \gamma_2 a_s - \gamma_1^3 c_s) \varepsilon^3 + \mathcal{O}(\varepsilon^4). \end{aligned} \quad (5.90)$$

Using definitions (5.85) and (5.86) for χ_1 and χ_2 respectively, we get after some algebraic manipulation:

$$x_f = \varepsilon x_0 + \mathbf{v} \varepsilon^3 + \mathcal{O}(\varepsilon^4), \quad (5.91)$$

where:

$$\begin{aligned} \mathbf{v} = & (c_1 - c_s + b_s a_s - b_s a_1) \gamma_1^3 + (e_s x_0 + e_1 x_0 - b_s b_1 x_0 - d_s F x_0 - d_s x_0) \gamma_1^2 + \\ & e(d_1 x_0^2 - d_s x_0^2) \gamma_1 + \frac{1}{2} \gamma_2 (F_2 - F_1) \langle \nabla H_u, x_0 \rangle. \end{aligned} \quad (5.92)$$

An explicit expression for \mathbf{v} in terms of the vector fields F_1, F_2 and F_s is not reported here for the sake of brevity. In the special case of linear vector fields, F_1, F_2, F_s , \mathbf{v} can be simplified to take the form:

$$\mathbf{v} = -\frac{1}{3} \frac{\langle \nabla H_u, x_0 \rangle^3}{\langle \nabla H_u, F_1 \rangle^2} \left(\frac{\partial F_1}{\partial x} + \frac{1}{2} (\langle \nabla H_u, F_2 \rangle - \langle \nabla H_u, F_1 \rangle) \right) (F_2 - F_1). \quad (5.93)$$

Substituting (3.15) for $\nabla H_u(x)$ allows to express the equation above as:

$$\mathbf{v} = \frac{2}{3} \frac{\langle \nabla H, \frac{\partial F_1}{\partial x} x_0 \rangle^3}{\langle \nabla H, F_2 \rangle \langle \nabla H, \frac{\partial F_1}{\partial x} F_1 \rangle^2} \left(\frac{\partial F_1}{\partial x} + \frac{1}{\langle \nabla H, F_2 \rangle} (\langle \nabla H, \frac{\partial F_1}{\partial x} F_1 \rangle - \langle \nabla H, \frac{\partial F_1}{\partial x} F_2 \rangle) \right) (F_2 - F_1). \quad (5.94)$$

In conclusion the normal-form map for a sliding bifurcation of type II can be written as:

$$D(x) = \begin{cases} \varepsilon x_0 & \text{if } \langle \nabla H_u, x_0 \rangle \leq 0 \\ \varepsilon x_0 + \varepsilon^3 \mathbf{v} + \mathcal{O}(\varepsilon^4) & \text{if } \langle \nabla H_u, x_0 \rangle > 0 \end{cases}, \quad (5.95)$$

where \mathbf{v} is given by (5.92).

5.4 Case IV: multisliding bifurcation

We have come now to the last of the four sliding bifurcation scenarios presented in Sec. 3. As shown in Fig. 7, in this case a segment of the system trajectory lying entirely on $\hat{\Sigma}$, hits *tangentially* the boundary of the sliding region, $\partial \hat{\Sigma}^-$ at the bifurcation point $x^* = 0$.

In order to construct the zero-time discontinuity mapping, we consider, as usual, the trajectory obtained by applying a perturbation of size ε to it, with ε sufficiently small. Such a trajectory is characterised by crossing the boundary $\partial \hat{\Sigma}$ at some point, say \bar{x} . The system then switches to flow F_1 , evolving above the switching manifold, until reaching it again at a point labelled $\hat{x} \in \hat{\Sigma}$.

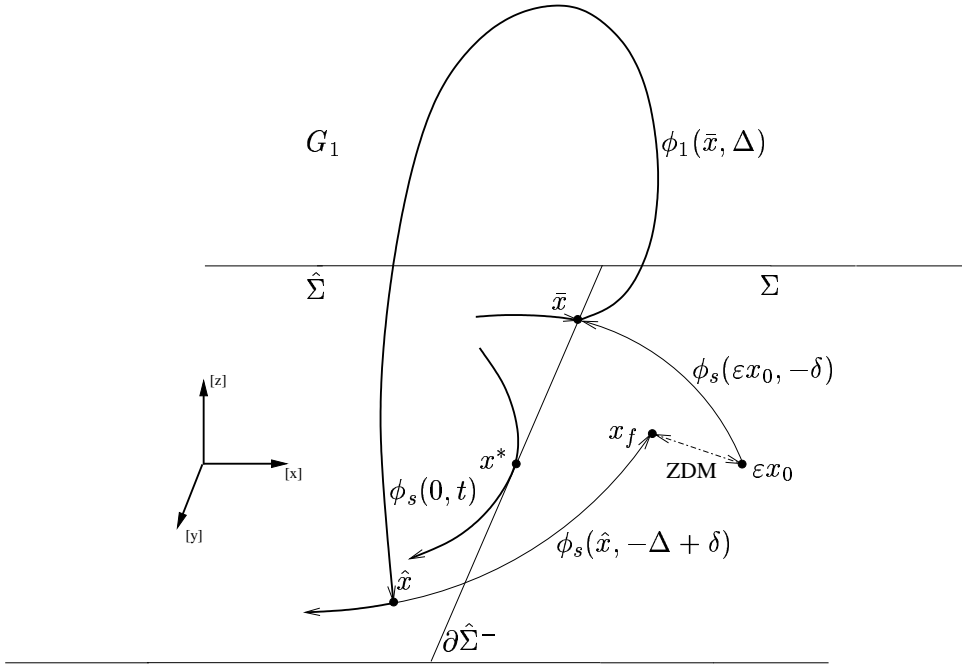


Figure 7: A schematic representation of constructing ZDM for multisliding bifurcation case

The ZDM in this case represents the correction that needs to be applied to the system flow, in order to allow the local description of the trajectory entirely in terms of the sliding flow ϕ_s . To derive such a mapping we need to consider three different steps (see Fig. 7): (i) we consider the perturbed trajectory assuming that it crosses the boundary of the sliding region at some time $t_1 = -\delta$; (ii) we evolve the system forward using flow ϕ_1 until it reaches the switching manifold, after some time, say Δ ; (iii) we flow the system using flow ϕ_s so that the total time spent flowing forward and backward is zero.

5.4.1 Step I

Let $x_m(t) = \phi_s(0, t)$ be the sliding trajectory undergoing a multisliding bifurcation at $x^* = 0$, $t^* = 0$ and let us consider perturbations of x_m of size ε given by:

$$x(t) = \phi_s(\varepsilon x_0, t) \quad (5.96)$$

for some x_0 which we assume to be such that:

$$\langle \nabla H_u, x_0 \rangle < 0. \quad (5.97)$$

As for the grazing-sliding case presented in Sec. 5.2 this condition ensures that the perturbed trajectory crosses $\partial\Sigma^-$ (twice) close to x^* .

At some time $t_1 = -\delta$ the trajectory, $x(t)$, crosses the boundary of the sliding region at $x = \bar{x}$. Using (5.26) we then obtain:

$$\begin{aligned} \bar{x} &= \phi_s(\varepsilon x_0, -\delta) \approx \varepsilon x_0 - \delta F_s + \delta^2 a_s - \varepsilon \delta b_s x_0 - \delta^3 c_s - \varepsilon^2 \delta d_s x_0^2 \\ &\quad + \varepsilon \delta^2 e_s x_0 + \delta^4 f_s - \varepsilon^3 \delta g_s x_0^3 + \varepsilon^2 \delta^2 h_s x_0^2 - \varepsilon \delta^3 j_s x_0. \end{aligned} \quad (5.98)$$

We defined δ as the time such that $H_u(\bar{x}) = 0$, thus, we have:

$$\langle \nabla H_u, \bar{x} \rangle = 0. \quad (5.99)$$

Hence, substituting (5.98) in (5.99) we obtain:

$$\begin{aligned} \varepsilon x_0 H_u - \delta F_s H_u + \delta^2 a_s H_u - \varepsilon \delta (b_s x_0) H_u - \delta^3 c_s H_u - \varepsilon^2 \delta (d_s x_0^2) H_u + \varepsilon \delta^2 (e_s x_0) H_u \\ + \delta^4 f_s H_u - \varepsilon^3 \delta (g_s x_0^3) H_u + \varepsilon^2 \delta^2 (h_s x_0^2) H_u - \varepsilon \delta^3 (j_s x_0) H_u \approx 0. \end{aligned} \quad (5.100)$$

The second term of (5.100), $-\delta\langle\nabla H_u, F_s\rangle$, is zero because of the general conditions for sliding bifurcations reported in Sec. 3.2. Thus, solving (5.100) for δ as an asymptotic expansion in $\sqrt{\varepsilon}$ yields:

$$\delta = \gamma_1\sqrt{\varepsilon} + \gamma_2\varepsilon + \gamma_3\varepsilon^{3/2} + \gamma_4(\varepsilon^2) + \mathcal{O}(\varepsilon^{5/2}). \quad (5.101)$$

where:

$$\gamma_1 = \sqrt{\frac{-x_0H_u}{a_sH_u}} = \sqrt{-2\frac{\langle\nabla H_u, x_0\rangle}{\langle\nabla H_u, \frac{\partial F_s}{\partial x}F_1\rangle}}, \quad (5.102)$$

$$\gamma_2 = \frac{1}{2}\frac{\gamma_1^2c_sH_u + (b_sx_0)H_u}{a_sH_u}, \quad (5.103)$$

$$\gamma_3 = \frac{1}{2}\frac{-\gamma_2^2a_sH_u - \gamma_1^2(x_0e_s)H_u + \gamma_2(b_sx_0)H_u + 3\gamma_1^2\gamma_2c_sH_u - \gamma_1^4f_sH_u}{\gamma_1a_sH_u}. \quad (5.104)$$

Note that for the sake of brevity, we omit the explicit expression for γ_4 which is particularly cumbersome and can be easily obtained by means of an algebraic manipulation software such as Maple or Mathematica. Conditions (3.24) and (5.97) guarantee that also in this case the asymptotic expansion performed is well defined.

Substituting (5.101)–(5.104) into (5.98), we obtain an expression for \bar{x} of the form:

$$\bar{x} = \chi_1\sqrt{\varepsilon} + \chi_2\varepsilon + \chi_3\varepsilon^{3/2} + \chi_4\varepsilon^2 + \mathcal{O}(\varepsilon^{5/2}), \quad (5.105)$$

where:

$$\chi_1 = -\gamma_1F_s, \quad (5.106)$$

$$\chi_2 = x_0 - \gamma_2F_s + \gamma_1^2a_s, \quad (5.107)$$

$$\chi_3 = -\gamma_3F_s + 2\gamma_1\gamma_2a_s - \gamma_1^3c_s - \gamma_1b_sx_0, \quad (5.108)$$

$$\chi_4 = (2\gamma_1\gamma_3 + \gamma_2^2)a_s - \gamma_2b_sx_0 + x_0\gamma_1^2e_s + \gamma_1^4f_s - \gamma_4F_s - 3\gamma_1^2\gamma_2c_s \quad (5.109)$$

5.4.2 Second step

We now study the motion of the trajectory after it leaves the sliding region at the point \bar{x} . The trajectory then follows flow ϕ_1 for some time, say Δ , until it reaches the next intersection with the switching manifold at the point $\hat{x} = \phi_1(\bar{x}, \Delta)$. Expanding the flow as a Taylor series about the origin, we can express \hat{x} as:

$$\begin{aligned} \hat{x} \approx & \bar{x} + \Delta F_1 + \Delta^2 a_1 + \Delta b_1 \bar{x} + \Delta^3 c_1 + \Delta d_1 \bar{x}^2 \\ & + \Delta^2 e_1 \bar{x} + \Delta^4 f_1 + \Delta g_1 \bar{x}^3 + \Delta^2 h_1 \bar{x}^2 + \Delta^3 j_1 \bar{x}. \end{aligned} \quad (5.110)$$

Since \hat{x} lies on the switching manifold we have:

$$\langle\nabla H, \hat{x}\rangle = 0. \quad (5.111)$$

Substituting (5.110) into (5.111) we then obtain to leading order:

$$\begin{aligned} & \bar{x}_H + \Delta F_{1H} + \Delta^2 a_{1H} + \Delta(b_1\bar{x})_H + \Delta^3 c_{1H} + \Delta(d_1\bar{x}^2)_H \\ & + (\Delta^2 e_1\bar{x})_H + \Delta^4 f_{1H} + \Delta(g_1\bar{x}^3)_H + \Delta^2(h_1\bar{x}^2)_H + \Delta^3(j_1\bar{x})_H = 0. \end{aligned} \quad (5.112)$$

Using the general conditions for sliding bifurcations reported in Sec. 3.2 and (3.21) together with the fact that \bar{x} lies on the switching manifold, it is trivial to show that the first three terms of (5.112) vanish. Moreover, since \bar{x} belongs to the boundary of the sliding region, we have $\langle\nabla H_u, \bar{x}\rangle = 0$. Using (3.15), this implies that the fourth term in (5.112) is also null.

After substituting for (5.105) into (5.112), we solve (5.112) for Δ as an asymptotic expansion in $\sqrt{\varepsilon}$. Ignoring the trivial solution $\Delta = 0$ we obtain:

$$\Delta = \nu_1 \sqrt{\varepsilon} + \nu_2 \varepsilon + \nu_3 \varepsilon^{3/2} + \nu_4 \varepsilon^2, \quad (5.113)$$

where:

$$\nu_1 = \frac{3c_{1H}\gamma_1 + c_{1H}\gamma_1 \sqrt{-3 + \frac{4(b_1 a_1)_H}{c_{1H}}}}{2c_{1H}}, \quad (5.114)$$

$$\nu_2 = \frac{-\nu_1((\chi_2 e_1)_{H\nu_1} + 2(\chi_1 \chi_2 d_1)_H + (\chi_1^3 g_1)_H + (\chi_1 j_1)_{H\nu_1^2} + \nu_1^3 f_{1H} + (\chi_1^2 h_1)_{H\nu_1})}{2(\chi_1 e_1)_{H\nu_1} + (\chi_1^2 d_1)_H + 3\nu_1^2 c_{1H}}, \quad (5.115)$$

$$\begin{aligned} \nu_3 = & \frac{-((e_1 \chi_1)_{H\nu_1^2} + 2(e_1 \chi_2)_{H\nu_1 \nu_2} + (e_1 \chi_3)_{H\nu_1^2} + 2(d_1 \chi_1 \chi_2)_{H\nu_2} + 2(d_1 \chi_1 \chi_3)_{H\nu_1}}{(2\chi_1 e_1)_{H\nu_1} + (\chi_1^2 d_1)_H + 3\nu_1^2 c_{1H}} \\ & + \frac{3g_{1H\nu_1} \chi_1^2 \chi_2 + (d_1 \chi_2^2)_{H\nu_1} + 3(j_1 \chi_1)_{H\nu_1^2} \nu_2 + (j_1 \chi_2)_{H\nu_1^3} + 3\nu_2^2 \nu_1 c_{1H}}{(2\chi_1 e_1)_{H\nu_1} + (\chi_1^2 d_1)_H + 3\nu_1^2 c_{1H}} \\ & + \frac{+\nu_2(g_1 \chi_1^3)_H + 4\nu_1^3 \nu_2 f_{1H} + 2(h_1 \chi_1^2)_{H\nu_1 \nu_2} + 2(h_1 \chi_1 \chi_2)_{H\nu_1^2}}{(2\chi_1 e_1)_{H\nu_1} + (\chi_1^2 d_1)_H + 3\nu_1^2 c_{1H}}. \end{aligned} \quad (5.116)$$

We omit for the sake of brevity the explicit expression for ν_4 which is particularly lengthy and does not add any extra information. (As mentioned earlier, this can be obtained by using any algebraic manipulation software.)

Note that, as discussed in Remark 1 in the Appendix, under the assumption that Σ and $\hat{\Sigma}$ can be flattened, applying (A.5) to (5.114) we obtain:

$$\nu_1 = 3\gamma_1. \quad (5.117)$$

Finally, after substituting (5.113) into (5.112) yields:

$$\hat{x} = \psi_1 \sqrt{\varepsilon} + \psi_2 \varepsilon + \psi_3 \varepsilon^{3/2} + \psi_4 \varepsilon^2 + \mathcal{O}(\varepsilon^{5/2}), \quad (5.118)$$

where:

$$\psi_1 = \chi_1 + \nu_1 F_1, \quad (5.119)$$

$$\psi_2 = \chi_2 + \nu_1 b_1 \chi_1 + \nu_2 F_1 + \nu_1^2 a_1, \quad (5.120)$$

$$\psi_3 = \nu_1 b_1 \chi_2 + \nu_2 b_1 \chi_1 + \nu_3 F_1 + \chi_3 + 2\nu_1 \nu_2 a_1 + \nu_1^3 c_1 + \chi_1^2 \nu_1 d_1 + \chi_1 \nu_1^2 e_1, \quad (5.121)$$

$$\begin{aligned} \psi_4 = & \nu_1 b_1 \chi_3 + \nu_2 b_1 \chi_2 + \nu_3 b_1 \chi_1 + (2\nu_1 \nu_3 + \nu_2^2) a_1 + \nu_4 F_1 + \nu_1 \chi_1^3 g_1 + 2\chi_1 \nu_1 \nu_2 e_1 + \\ & + \chi_2 \nu_1^2 e_1 + \chi_1 \nu_1^3 j_1 + (\chi_1^2 \nu_2 + 2\chi_1 \chi_2 \nu_1) d_1 + \chi_4 + \chi_1^2 \nu_1^2 h_1 + 3\nu_1^2 \nu_2 c_1 + \nu_4 F_1. \end{aligned} \quad (5.122)$$

5.4.3 Third step

The last step describes the evolution of the trajectory from \hat{x} to $x_f = \phi_s(\hat{x}, \delta - \Delta)$. We use again Taylor expansion evaluated at the bifurcation point to obtain an approximate expression for x_f . Thus, we have:

$$\begin{aligned} x_f \approx & \hat{x} + (\delta - \Delta) F_s + (\delta - \Delta)^2 a_s + (\delta - \Delta) b_s \hat{x} + (\delta - \Delta)^3 c_s + \hat{x}^2 (\delta - \Delta) d_s \\ & + \hat{x} (\delta - \Delta)^2 e_s + (\delta - \Delta)^4 f_s + \hat{x}^3 (\delta - \Delta) g_s + (\delta - \Delta)^2 h_s \hat{x}^2 + \hat{x} (\delta - \Delta)^3 j_s. \end{aligned} \quad (5.123)$$

Substituting (5.101), (5.105), (5.110) and (5.113) into (5.123), we can obtain an expression for x_f in terms of the initial perturbation ε . Collecting terms at subsequent powers of ε yields the following expression for x_f to leading order:

$$x_f = \xi_1 \sqrt{\varepsilon} + \xi_2 \varepsilon + \xi_3 \varepsilon^{3/2} + \xi_4 \varepsilon^2 + \mathcal{O}(\varepsilon)^{5/2} \quad (5.124)$$

where

$$\xi_1 = (\chi_1 + \gamma_1 F), \quad (5.125)$$

$$\begin{aligned} \xi_2 = & (\chi_2 + \nu_1^2 a_1 + \nu_2 F + \nu_1 b_1 \chi_1 + \\ & (\chi_1 + \nu_1 F)(\gamma_1 - \nu_1) b_s + (\gamma_1 - \nu_1)^2 a_s + (\gamma_2 - \nu_2) F), \end{aligned} \quad (5.126)$$

and expressions for ξ_3 and ξ_4 are reported in the Appendix.

Substituting (5.106), (5.107) and (5.117) into (5.125, 5.126), we can show that $\xi_1 = 0$ and:

$$\xi_2 = x_0 + \gamma_1^2 a_s + \gamma_1^2 a_1 - \gamma_1^2 b_1 F_s. \quad (5.127)$$

Eq. (5.127) can be further simplified considering that at the bifurcation point $F_s = F_1$ and thus, as shown in the Appendix (Remark 1), $a_1 = a_s$. Moreover, from the definitions of the coefficients of the Taylor expansion (5.26), it follows that $b_s F = 2a_s = 2a_1$. Thus, (5.127) reduces to $\xi_2 = x_0$.

To obtain the leading order term of the local mapping we need to find an expression for the first non-vanishing term of x_f . The next term under consideration stands at $\varepsilon^{3/2}$ in (5.124) and is characterised by the coefficient ξ_3 . This can also be shown to vanish to zero (see Remark 3 in the Appendix). Thus, to leading order the correction to be made to εx_0 in order to account for the presence of the switching manifold (the ZDM) is at least of order $\mathcal{O}(\varepsilon^2)$. Remark 4 in the Appendix contains an explicit expression for this term and its coefficient ξ_4 .

Having established the leading-order term of the ZDM for the multisliding bifurcation case, the general form of the map can be written as:

$$D(x_0) = \begin{cases} \varepsilon x_0 & \text{if } \langle \nabla H_u, x_0 \rangle \geq 0, \\ \varepsilon x_0 + \varepsilon^2 \xi_4 + \mathcal{O}(\varepsilon^{5/2}) & \text{if } \langle \nabla H_u, x_0 \rangle < 0. \end{cases} \quad (5.128)$$

where, as mentioned above, the explicit expression for ξ_4 in general case is reported in the Appendix.

We will present here the resulting expression for ξ_4 in the case of Piecewise Linear vector fields F_1 , F_2 and their constant difference. After lengthy algebraic manipulations the resulting expression yields:

$$\xi_4 = \frac{9}{4} \frac{\langle \nabla H_u, x_0 \rangle^2}{\langle \nabla H_u, \frac{\partial F_1}{\partial x} F_1 \rangle} \frac{\partial F_1}{\partial x} (F_2 - F_1) + \frac{9}{8} \frac{\langle \nabla H_u, x_0 \rangle^2}{\langle \nabla H_u, \frac{\partial F_1}{\partial x} F_1 \rangle} \langle \nabla H_u, F_2 \rangle (F_2 - F_1), \quad (5.129)$$

which is non-zero if non-standard cancellation occurs. Substituting in (5.129) for ∇H_u (3.15) yields the above equation to take the form:

$$\xi_4 = -\frac{9}{2} \frac{\langle \nabla H, \frac{\partial F_1}{\partial x} x_0 \rangle^2}{\langle \nabla H, F_2 \rangle \langle \nabla H, (\frac{\partial F_1}{\partial x})^2 F_1 \rangle} \left(\frac{\partial F_1}{\partial x} - \frac{\langle \nabla H, \frac{\partial F_1}{\partial x} F_2 \rangle}{\langle \nabla H, F_2 \rangle} \right) (F_2 - F_1). \quad (5.130)$$

6 A representative example: relay feedback systems

We use a three-dimensional representative example to give numerical confirmation of the results presented in the paper. Specifically, we study the normal form maps of sliding bifurcations in the three-dimensional relay feedback system analysed in [20, 26, 27]. In so doing, we perform a comparison between analytical normal form maps and numerically computed ones.

Third order system. Matrix representation

We consider a third order relay feedback system having the following state-space representation:

$$\begin{aligned} \dot{x} &= Ax + Bu, \\ u &= -\text{sgn}(y), \\ y &= Cx, \end{aligned} \quad (6.131)$$

where:

$$A = \begin{pmatrix} -(2\zeta\omega + \lambda) & 1 & 0 \\ -(2\zeta\omega\lambda + \omega^2) & 0 & 1 \\ -\lambda\omega^2 & 0 & 0 \end{pmatrix}, \quad B = \begin{pmatrix} k \\ 2k\sigma\rho \\ k\rho^2 \end{pmatrix}, \quad C = \begin{pmatrix} 1 \\ 0 \\ 0 \end{pmatrix}^T. \quad (6.132)$$

Thus, vector fields F_1 and F_2 may be written as:

$$F_1 = Ax - B, \quad F_2 = Ax + B.$$

Applying Utkin's equivalent control method we can express the vector field F_s governing the flow on the switching manifold as:

$$F_s = A_s x,$$

where A_s can be expressed as:

$$A_s = \begin{pmatrix} 0 & 0 & 0 \\ 0 & -2\sigma\rho & 1 \\ 0 & -\rho^2 & 0 \end{pmatrix}. \quad (6.133)$$

In the case considered $H(x) = Cx$ and $H_u(x) = -\frac{CAx}{CB}$. Hence, the switching manifold is defined as:

$$\Sigma := \{x \in \mathbb{R}^3 : Cx = 0\} \quad (6.134)$$

where the boundary of the sliding region is given by:

$$\partial\Sigma^\pm := \{x \in H : -\frac{CAx}{CB} = \pm 1\}. \quad (6.135)$$

The dynamics of the system presented has been extensively studied numerically in [20, 26, 27]. We shall note here that the sliding bifurcation type I, the grazing-sliding bifurcation and the multisliding bifurcation have been detected in this system but no evidence of switching-sliding bifurcation has been found. In what follows we will present the local mappings for these three cases of sliding bifurcations using numerical simulations. We will compare numerical results with analytical expressions obtained using the results presented in Sec. 5.

In general, the bifurcations mentioned above occur in the relay system under investigation at points $x^* = (x_1^*, x_2^*, x_3^*) \neq 0$. Since, our analytical derivation requires the bifurcation point to be located at $x^* = 0$, in order to compare numerical and analytical results an appropriate transformation of the matrices A , B and C needs to be applied. After translating the bifurcation point x^* to the origin, the matrices A , B , C take the form:

$$A' = \begin{pmatrix} -(2\zeta\omega + \lambda) & 1 & 0 \\ -(2\zeta\omega\lambda + \omega^2) & 0 & 1 \\ -\lambda\omega^2 & 0 & 0 \end{pmatrix}, \quad B'_1 = \begin{pmatrix} 0 \\ -2k\sigma\rho + x_3^* \\ -k\rho^2 \end{pmatrix}, \quad B'_2 = \begin{pmatrix} 2k \\ 2k\sigma\rho + x_3^* \\ k\rho^2 \end{pmatrix}. \quad (6.136)$$

$$C' = (1 \ 0 \ 0), \quad (6.137)$$

The applied transformation causes matrices B'_1, B'_2 to have a different form for the transformed vector fields F'_1 and F'_2 , but the matrices A, C stay the same for both vector fields i.e.: $F'_1 = A'x + B'_1, F'_2 = A'x + B'_2$. We need to apply the same transformation to the vector field F_s governing the sliding motion. After that we get a new vector field governing the sliding flow: $F'_s = A'_s x + B'_s$ where:

$$A'_s = \begin{pmatrix} 0 & 0 & 0 \\ 0 & -2\sigma\rho & 1 \\ 0 & -\rho^2 & 0 \end{pmatrix}, \quad B'_s = \begin{pmatrix} 0 \\ -2k\sigma\rho + x_3^* \\ -k\rho^2 \end{pmatrix} \quad (6.138)$$

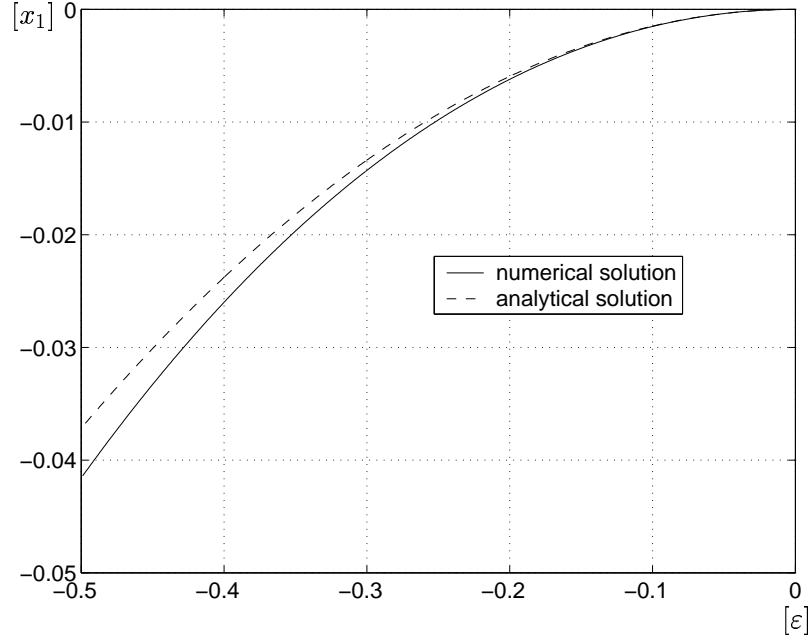


Figure 8: ZDM for sliding bifurcation type I after subtracting identity term

Having transformed the system under consideration in such a way that the bifurcation point x^* is located at the origin, we can now compare analytical expressions of the ZDM derived in Sec. 5 with numerical results. In what follows, we will derive analytical forms of the ZDM for all the four cases of sliding bifurcations. We will then validate the analytical results numerically for the three bifurcation scenarios detected in the relay system under investigation.

6.1 Sliding bifurcation type I

The ZDM in the case of relay feedback system can be obtained from (5.46) after substituting expressions defining vector fields F'_1, F'_2 into (5.48). Thus, the ZDM can be written as:

$$D(x) = \begin{cases} x & \text{for } C'A'x \geq 0 \\ x + \frac{1}{2} \frac{(C'A'x)^2}{(C'B'_2)(C'A'B'_1)} (B'_2 - B'_1) + H.O.T & \text{for } C'A'x < 0. \end{cases} \quad (6.139)$$

Following [26], we consider the sliding bifurcation type I observed in the circuit when $\omega = \lambda = k = -\sigma = 1$, $\rho \approx 2.09885$, at the point $x^* = [0 \ 1 \ 9.924404784]^T$. We can now compare the analytical mapping (6.139) with numerical data. To do so we plot how an arbitrarily chosen coordinate of some final point scales as the initial conditions are perturbed by an amount ε from the origin. It should be noted here that it suffices to vary one coordinate of the initial point so as the condition $C'A'x < 0$ is satisfied. Since, the identity term of the ZDM in figure (8) has been subtracted *a fortiori*, the analytical curve converges to 0 at the bifurcation point.

We can see in Fig. 8, that the numerical and analytical curves do converge asymptotically, confirming our analytical predictions.

6.2 Grazing sliding bifurcation

We consider now the grazing-sliding detected for $-\sigma = \rho = k = 1$, $\lambda = 0.05$, $\zeta = 0.0485$, occurring at the point: $x^* = [0 \ 1 \ -1.84481226874003]^T$. Using the results of Sec. 5.2, the ZDM in this case has the form:

$$D(x) = \begin{cases} x & \text{for } C'x \geq 0, \\ x - \frac{C'x}{C'B'_2} (B'_2 - B'_1) + \mathcal{O}(x^{3/2}) & \text{for } C'x < 0 \end{cases} \quad (6.140)$$

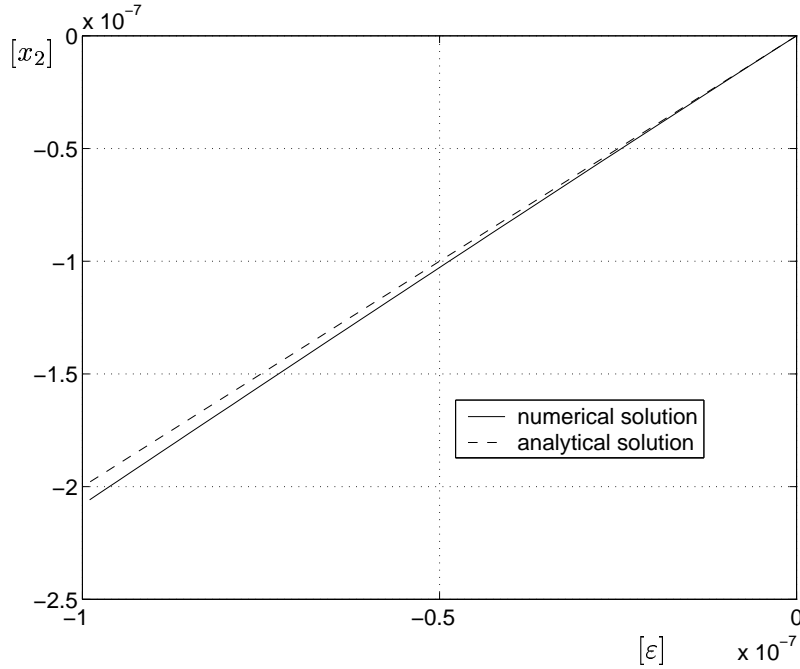


Figure 9: ZDM after subtracting identity term for grazing-sliding bifurcation, plotted x_2 coordinate versus x_1 coordinate

As for the previous case, the numerical and analytical data are compared after subtracting the identity from the ZDM. The comparison between numerical and analytical data is presented in Fig. (9).

Again we see a good agreement between the analytical predictions and the numerical simulations. Our numerics confirm that the mapping has indeed a leading-order linear behaviour locally to the bifurcation point.

6.3 Multisliding bifurcation in the relay feedback system

We move now to the case of multisliding bifurcations. As reported in [26], a multisliding bifurcation is observed in the relay system considered, when $\lambda = k = -\sigma = \rho = 1$, $\zeta = 0.05$, $\omega = 10.24176$ and takes place at the point: $x^* = [0 \ 1 \ -2]^T$. Using the results of Sec. 5.4, the ZDM takes the form:

$$D(x) = \begin{cases} x & \text{for } C'A'x \leq 0, \\ x - \frac{9}{2} \frac{(C'A'x)^2}{(C'B'_2)(C'A'A'B'_1)} \left(A' - \frac{C'A'B'_2}{C'B'_2} \right) (B'_2 - B'_1) + \mathcal{O}(x^{5/2}) & \text{for } C'A'x > 0. \end{cases} \quad (6.141)$$

In Fig. (10), we see that the analytical and numerical curves converge asymptotically, confirming the quadratic nature of the multisliding normal form map.

6.4 Sliding bifurcation type II

Finally, we come to sliding bifurcations type II. These events have not been observed in relay feedback systems. Thus, we limit our presentation to the derivation of the ZDM for this bifurcation event using the results of Sec. 5.3. Specifically, we get:

$$D(x) = \begin{cases} x & \text{for } C'A'x \leq 0 \\ x + \frac{2}{3} \frac{(C'A'x)^3}{(C'B'_2)(C'A'B'_1)^2} \left(A' + \frac{C'A'B'_1 - C'A'B'_2}{C'B'_2} \right) (B'_2 - B'_1) + \mathcal{O}(x^4) & \text{for } C'A'x > 0. \end{cases} \quad (6.142)$$

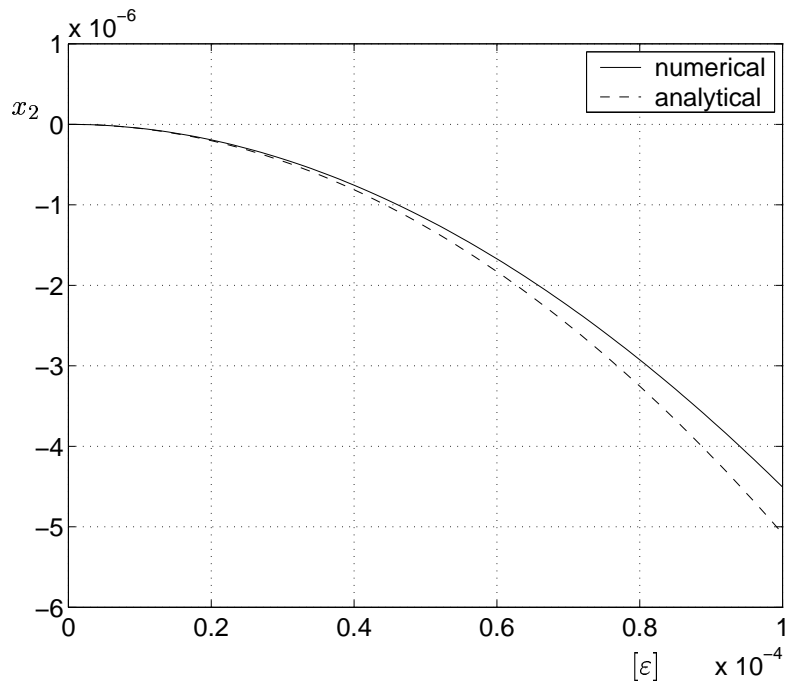


Figure 10: ZDM for multislider bifurcation (after subtracting identity mapping) - range of perturbation: $10^{-6} - 10^{-4}$

The numerical validation of this map is currently under investigation and will be reported elsewhere.

7 General Remarks

In Sec. 5 we have derived expressions for the zero time discontinuity mappings in the four cases of sliding bifurcations. We have shown that the discontinuity mappings consist of two different expressions on either side of a boundary, with a degree of continuity across the boundary that varies for the different cases. In [32] we will show how these discontinuities translate into discontinuities in the Poincaré mapping for a given periodic orbit. Here we shall mention that generally the type of discontinuity is preserved under compositions with a smooth mappings. Thus, the type of discontinuity found in the ZDM describing particular bifurcation scenario will characterise the full Poincaré map.

Since, we have found that in the grazing-sliding case the ZDM has a piecewise linear character there is a possibility of a sudden bifurcation as an hyperbolic orbit crosses the discontinuity boundary. Since the Poincaré map in this case has a discontinuous Jacobian, the possible bifurcation scenarios following grazing-sliding can be classified using techniques developed for piecewise-linear maps (see [16, 8]).

In all the other three cases, dramatic bifurcation scenarios should be expected for non-hyperbolic orbits. This would then typically be a co-dimension 2 bifurcation, as one parameter is needed to make the orbit non-hyperbolic, and another to make it encounter the discontinuity.

Nevertheless, if the discontinuity in the Poincaré mapping, say in the second derivative, is large in magnitude, sliding bifurcations can organise secondary bifurcations. For example, a saddle-node bifurcation is often observed in numerical simulations as the parameters are further varied from a multislider bifurcation point (see [26]).

These and other issues will be discussed in detail in [32].

8 Conclusions

We have discussed the characterisation of novel bifurcations in dynamical systems with sliding. In particular, using so-called discontinuity mappings, we derived normal form maps for each of the four possible scenarios involving interactions of system trajectories with the sliding region. To obtain analytical leading-order approximations for such mappings, we performed a combination of Taylor series expansions and asymptotics.

We showed that the leading order term of the local map is quadratic for the sliding bifurcation type I and multisliding bifurcation, or cubic in the case of sliding bifurcation type II. In the grazing-sliding bifurcation case the normal form map has a piecewise linear character. Thus, as shown in [8, 9, 16] if grazing-sliding bifurcation occurs in the system a wide range of dynamical behaviour may be observed, including sudden jumps to chaos and period-adding bifurcations.

We also discussed how the normal form mappings can be used to analyse the behaviour of periodic orbits undergoing sliding bifurcations. We should mention here that analysis presented in this paper captures the dynamics associated with trajectories that are in the close vicinity of the bifurcating trajectory. Global analysis of periodic orbits still remains an open issue.

Further work shall be directed towards a consistent classification of the possible bifurcations exhibited by the maps derived in this paper. Ongoing research is devoted to the analysis of sliding bifurcations in systems of relevance in applications.

A Appendix

A.1 Remark 1

An important result follows from the assumption that Σ and $\partial\hat{\Sigma}$ can be considered linear. Specifically, assuming Σ to be linear we get:

$$\frac{\partial^2 H_u}{\partial x^2} = 0. \quad (\text{A.1})$$

Substituting for $\frac{\partial H_u}{\partial x}$, (3.15) we get:

$$\frac{\partial^2 H_u}{\partial x^2} = -2 \frac{\partial}{\partial x} \left(\frac{\partial H}{\partial x} \frac{\partial F_1}{\partial x} \right). \quad (\text{A.2})$$

Differentiating (A.2) yields:

$$\frac{\partial^2 H_u}{\partial x^2} = 2 \frac{-\frac{\partial^2 H}{\partial x^2} \frac{\partial F_1}{\partial x} \frac{\partial H}{\partial x} F_2 - \frac{\partial H}{\partial x} \frac{\partial^2 F_1}{\partial x^2} \frac{\partial H}{\partial x} F_2 + \frac{\partial^2 H}{\partial x^2} F_2 \frac{\partial H}{\partial x} \frac{\partial F_1}{\partial x} + \frac{\partial H}{\partial x} \frac{\partial F_2}{\partial x} \frac{\partial H}{\partial x} \frac{\partial F_1}{\partial x}}{\langle \nabla H, F_2 \rangle^2} \quad (\text{A.3})$$

Both the first and the third term in the numerator of equation (A.3) are 0 since, $\frac{\partial^2 H}{\partial x^2} = 0$. Thus, since the denominator of (A.3) is positive, (A.1) yields:

$$\nabla H \left(\frac{\partial F_2}{\partial x} \nabla H \frac{\partial F_1}{\partial x} - \frac{\partial^2 F_1}{\partial x^2} \langle \nabla H, F_2 \rangle \right) = 0. \quad (\text{A.4})$$

Rearranging (A.3) we can get that if $\partial\hat{\Sigma}$ is flat, the following must hold:

$$\nabla H \frac{\partial^2 F_1}{\partial x^2} = \frac{1}{\langle \nabla H, F_2 \rangle} \left(\nabla H \frac{\partial F_2}{\partial x} \nabla H \frac{\partial F_1}{\partial x} \right). \quad (\text{A.5})$$

A.2 Remark 2

This remark is valid for the *multisliding bifurcation* case. The general condition for all the sliding bifurcations ensure that at the bifurcation point $F_s = F_1$. Thus, in the multisliding bifurcation case terms denoted as a_1, a_s take the same value. Let us express a_s as:

$$a_s = \frac{1}{2} \left(\frac{\partial F_1}{\partial x} F_s + \frac{1}{2} \left(F_2 \langle \nabla H_u, F_s \rangle - F_1 \langle \nabla H_u, F_s \rangle \right) \right). \quad (\text{A.6})$$

We can simplify a_s so that (A.6) takes the form:

$$a_s = \frac{1}{2} \frac{\partial F_1}{\partial x} F_s. \quad (\text{A.7})$$

Since $a_s = \frac{1}{2} \frac{\partial F_1}{\partial x} F_s$, $a_1 = \frac{1}{2} \frac{\partial F_1}{\partial x} F_1$ and $F_s = F_1$, this implies that $a_s = a_1$.

A.3 Remark 3

In what follows, we present the general expression for the term denoted as ξ_3 in equation (5.124). To get an expression for ξ_3 we will substitute (5.110), (5.101), (5.113), (5.105) into (5.123). Since $F_s = F_1$ we shall refer to the vector field F_1 when the vector field F without a subscript is used. Thus, ξ_3 has the form:

$$\begin{aligned} \xi_3 = & ((\gamma_3 - \nu_3)F + \chi_3 + 2\nu_1\nu_2a_1 + \chi_1\nu_1^2e_1 + \chi_1^2\nu_1d_1 + 2(\gamma_1 - \nu_1)(\gamma_2 - \nu_2)a_s + \nu_1^3c_1 + \nu_1b_1\chi_2 + \\ & + \nu_2b_1\chi_1 + (\gamma_1 - \nu_1)^3c_s + ((\chi_1 + \nu_1F)(\gamma_2 - \nu_2) + (\chi_2 + \nu_1^2a_1 + \nu_2F + \nu_1b_1\chi_1)(\gamma_1 - \nu_1))b_s + \\ & + \nu_3F + (\chi_1 + \nu_1F)(\gamma_1 - \nu_1)^2e_s + (\chi_1 + \nu_1F)^2(\gamma_1 - \nu_1)d_s)\varepsilon^{3/2}. \end{aligned} \quad (\text{A.8})$$

We can simplify the equation above using the fact that $a_1 = a_s$; and substituting for (5.106), (5.107), (5.109) χ_1, χ_2, χ_3 subsequently. From Taylor expansion it also follows that: $d_sF^2 = 3c_s - b_s a_s$, $d_1F^2 = 3c_1 - b_1 a_1$, $e_sF = 3c_s$, $e_1F = 3c_1$. Thus, after lengthy algebraic manipulations, (A.8) takes the form:

$$\begin{aligned} \xi_3 = & (-3b_1\gamma_2F + 4b_s\gamma_2F + 4a_s\nu_2 - 2\gamma_2a_s + 3b_1x_0 + 6\nu_2a_1 - 3b_sx_0 - 4b_sF\nu_2 - F\nu_2b_1)\gamma_1 + \\ & + (6Fb_s b_1 + 9c_1 + 6b_s a_s - 18a_1 b_s - 9c_s - 3b_1 a_1 + 3a_s b_1)\gamma_1^3. \end{aligned} \quad (\text{A.9})$$

Finally, after further simplifications and using the fact that $\nu_1 = 3\gamma_1$, $b_sF = 2a_1$, $b_1F = 2a_1$ (A.9) can be rewritten as:

$$\xi_3 = 9(c_1 - c_s)\gamma_1^3 + (3b_1x_0 - 3b_sx_0)\gamma_1. \quad (\text{A.10})$$

Using the fact that $\gamma_1^2 = -2 \frac{\langle \nabla H_u, x_0 \rangle}{\langle \nabla H_u, \frac{\partial F_1}{\partial x} F_1 \rangle}$ and substituting for c_s, c_1, b_s, b_1 the elements of

Taylor expansion (5.26). Then, we get:

$$\begin{aligned} \xi_3 = & -3\gamma_1 \left(\frac{\langle \nabla H_u, x_0 \rangle}{\langle \nabla H_u, \frac{\partial F_1}{\partial x} F_1 \rangle} \frac{\partial^2 F_1}{\partial x^2} F_1^2 + \frac{\langle \nabla H_u, x_0 \rangle}{\langle \nabla H_u, \frac{\partial F_1}{\partial x} F_1 \rangle} \left(\frac{\partial F_1}{\partial x} \right)^2 F_1 + \right. \\ & \left. - \left(\frac{\langle \nabla H_u, x_0 \rangle}{\langle \nabla H_u, \frac{\partial F_1}{\partial x} F_1 \rangle} \frac{\partial^2 F_s}{\partial x^2} F_s^2 + \frac{\langle \nabla H_u, x_0 \rangle}{\langle \nabla H_u, \frac{\partial F_1}{\partial x} F_1 \rangle} \left(\frac{\partial F_s}{\partial x} \right)^2 F_s \right) + \frac{\partial F_1}{\partial x} x_0 - \frac{\partial F_s}{\partial x} x_0 \right). \end{aligned} \quad (\text{A.11})$$

Expression (A.11) can be shown to be identically nought, noting that:

1. $\frac{\partial F_s}{\partial x} = \frac{\partial F_1}{\partial x} + \frac{1}{2}F_2\nabla H_u - \frac{1}{2}F_1\nabla H_u,$
2. $\frac{\partial^2 F_s}{\partial x^2} = \frac{\partial^2 F_1}{\partial x^2} + \frac{1}{2}\left(\frac{\partial F_2}{\partial x}\nabla H_u + \frac{\partial^2 H_u}{\partial x}F_2 - \frac{\partial F_1}{\partial x}\nabla H_u - \frac{\partial^2 H_u}{\partial x}F_1\right),$
3. $\left(\frac{\partial F_s}{\partial x}\right)^2 F = \left(\frac{\partial F_1}{\partial x}\right)^2 F + \frac{1}{2}\left(F_2\nabla H_u\frac{\partial F_1}{\partial x}F_1 - F_1\nabla H_u\frac{\partial F_1}{\partial x}F_1\right).$

Since the above substitutions simplify (A.11) to nought the local map in the multisliding bifurcation case does not contain terms of $O(\varepsilon^{3/2})$.

A.4 Remark 4

To get an expression for ξ_4 , in (5.124) where ξ_4 appears, we substitute (5.105), (5.110), (5.101), (5.113) into (5.123). The resulting expression yields:

$$\begin{aligned} \xi_4 = & \psi_4 + (\psi_1(\gamma_3 - \nu_3) + \psi_2(\gamma_2 - \nu_2) + \psi_3(\gamma_1 - \nu_1))b_s + (2(\gamma_1 - \nu_1)(\gamma_3 - \nu_3) + (\gamma_2 - \nu_2)^2)a_s + \\ & (\gamma_4 - \nu_4)F + (2\psi_1(\gamma_1 - \nu_1)(\gamma_2 - \nu_2) + \psi_2(\gamma_1 - \nu_1)^2)e_s + (\gamma_1 - \nu_1)^4 + g_s(\gamma_1 - \nu_1)\psi_1^3 + \\ & 3(\gamma_1 - \nu_1)^2(\gamma_2 - \nu_2)c_s + h_s(\gamma_1 - \nu_1)^2\psi_1^2 + j_s\psi_1(\gamma_1 - \nu_1)^3. \end{aligned} \tag{A.12}$$

After substituting (5.106) - (5.109), (5.119) - (5.122) for $\chi_1, \chi_2, \chi_3, \chi_4, \psi_1, \psi_2, \psi_3, \psi_4$ we can get the final expression for ξ_4 .

References

- [1] B. Brogliato. *Nonsmooth Mechanics*. Springer–Verlag, 1999.
- [2] M. Oestreich N. Hinrichs and K. Popp. On the modelling of friction oscillators. *Journal of Sound and Vibration*, 216(3):435–459, 1998.
- [3] M. di Bernardo, F. Garofalo, L. Glielmo, and F. Vasca. Switchings, bifurcations and chaos in DC/DC converters. *IEEE Transactions on Circuits and Systems, Part I*, 45:133–141, 1998.
- [4] M. di Bernardo and F. Vasca. On discrete time maps for the analysis of bifurcations and chaos in DC/DC converters. *IEEE Transactions on Circuits and Systems, Part I*, 47:130–143, 2000.
- [5] M. di Bernardo, A. R. Champneys, and C. J. Budd. Grazing, skipping and sliding: analysis of the nonsmooth dynamics of the DC/DC buck converter. *Nonlinearity*, 11:858–890, 1998.
- [6] J.H.B. Deane and D.C. Hamill. Analysis, simulation and experimental study of chaos in the buck converter. In *Proceedings of the Power Electronics Specialists Conf. (PESC 1990)*, pages 491–8, New York, IEEE Press, 1990.
- [7] A.J. Van der Schaft and J.M. Schumacher. *An introduction to Hybrid Dynamical Systems*. Springer - Verlag, 2000.
- [8] L. E. Nusse and J. A. Yorke. Border–collision bifurcations for piece-wise smooth one-dimensional maps. *International Journal of Bifurcation and Chaos*, 5:189–207, 1995.
- [9] L. E. Nusse and J. A. Yorke. Border-collision bifurcations including ‘period two to period three’ for piecewise smooth systems. *Physica D*, 57:39–57, 1992.

- [10] L. E. Nusse and J. A. Yorke. Border collision bifurcation: an explanation for observed bifurcation phenomena. *Physical Review E*, 49:1073–1076, 1994.
- [11] A. B. Nordmark. Non-periodic motion caused by grazing incidence in impact oscillators. *Journal of Sound and Vibration*, 2:279–297, 1991.
- [12] M. I. Feigin. Doubling of the oscillation period with c -bifurcations in piecewise continuous systems. *PMM*, 34:861–869, 1970.
- [13] M. I. Feigin. On the generation of sets of subharmonic modes in a piecewise continuous system. *PMM*, 38:810–818, 1974.
- [14] M. I. Feigin. On the structure of C -bifurcation boundaries of piecewise continuous systems. *PMM*, 42:820–829, 1978.
- [15] M. di Bernardo, C.J. Budd, and A.R. Champneys. Unified framework for the analysis of grazing and border-collisions in piecewise-smooth systems. *Physical Review Letters*, 86(12):2554–2556, 2001.
- [16] M. di Bernardo, M.I. Feigin, S.J. Hogan, and M.E. Homer. Local analysis of C -bifurcations in n -dimensional piecewise smooth dynamical systems. *Chaos, Solitons and Fractals*, 10:1881–1908, 1999.
- [17] S. Banerjee and C. Grebogi. Border collision bifurcations in two-dimensional piecewise smooth maps. *Physical Review E*, 59:4052–4061, 1999.
- [18] A.F. Filippov. *Differential equations with discontinuous righthand sides*. Kluwer, Dordrecht, 1988.
- [19] V. I. Utkin. *Sliding Modes in Control Optimization*. Springer-Verlag, Berlin, 1992.
- [20] M. di Bernardo, K.H. Johansson, and F. Vasca. Self-oscillations in relay feedback systems: Symmetry and bifurcations. *International Journal of Bifurcations and Chaos*, (4), 2001.
- [21] S. Jaguste K.M. Moudgalya. A class of discontinuous dynamical systems i. an ideal gas-liquid system. *Chemical Engineering Science*, 56:3595–3609, 2001.
- [22] S. Jaguste K.M. Moudgalya. A class of discontinuous dynamical systems ii. an industrial slurry high density polyethylene reactor. *Chemical Engineering Science*, 56:3611–3621, 2001.
- [23] K. Popp and P. Shelter. Stick–slip vibrations and chaos. *Philosophical Transactions of the Royal Society A*, 332(1624):89–105, 1990.
- [24] M. I. Feigin. *Forced Oscillations in systems with discontinuous nonlinearities*. Nauka, Moscow, 1994. In Russian.
- [25] J.S. Fedosenko and M.I. Feigin. On the theory of the slipping state in dynamical systems with collisions. *PMM*, 36(5):840 – 850, 1972.
- [26] P. Kowalczyk and M. di Bernardo. On a novel class of bifurcations in hybrid dynamical systems - the case of relay feedback systems. In *Proceeding of Hybrid Systems Computation and Control*. Springer–Verlag, 2001.
- [27] P. Kowalczyk and M. di Bernardo. Existence of stable asymmetric limit cycles and chaos in unforced symmetric relay feedback systems. In *Proceedings of European Control Conference, Porto*, 2001.

- [28] H. Dankowicz and A.B. Nordmark. On the origin and bifurcations of stick-slip oscillations. *Physica D*, 136:280–302, 1999.
- [29] C.J. Budd M. di Bernardo and A.R. Champneys. Normal form maps for grazing bifurcations in n-dimensional piecewise-smooth dynamical systems. *to appear in Physica D*, 2001.
- [30] M. di Bernardo, C.J. Budd, and A. R. Champneys. Corner–collision implies border–collision bifurcation. *Physica D*, 154:171 – 194, 2001.
- [31] M.H. Fredriksson and A.B. Nordmark. On normal form calculations in impact oscillators. *Proc. Royal Soc. London A*, 456:315–329, 2000.
- [32] M. di Bernardo, P.Kowalczyk, and A.Nordmark. Classification of sliding bifurcations of periodic orbits in piecewise smooth dynamical systems. in preparation, 2002.